1972

Simulation of a Surface Thermal Anomaly

Corwyn Richard Meyer

SIMULATION OF A SURFACE THERMAL ANOMALY

BY

CORWYN RICHARD MEYER

A thesis submitted
in partial fulfillment of the requirements for the
degree Master of Science, Major in
Physics, South Dakota
State University

1972

SIMULATION OF A SURFACE THERMAL ANOMALY

This thesis is approved as a creditable and independent investigation by a candidate for the degree, Master of Science, and is acceptable for meeting the thesis requirements for this degree. Acceptance of this thesis does not imply that the conclusions reached by the candidate are necessarily the conclusions of the major department.

Thesis Adviser / Date

Head, Physics Department Date

ACKNOWLEDGMENTS

The author wishes to express his appreciation to Dr. Tunheim for his guidance in the research and preparation of this thesis and to Dr. Duffey for his guidance throughout the author's graduate work.

The author also wishes to express his appreciation to Mr. Myers, Director of the Remote Sensing Institute and to Dr. Moore for enabling this research to be conducted. The work was performed under USGS Grant 14-08-0001-12510 with additional computer time supplied by the Computing Center.

The author is grateful to Dr. Lumsdaine and Dr. Horton for their inspiring comments and to Mrs. Nesson for her assistance in the development of the computer programs used.

CRM

TABLE OF CONTENTS

LIST OF FIGURES

LIST OF TABLES

Table

Page

CHAPTER 1. INTRODUCTION

The demand for good quality water is rapidly increasing as the result of intensified agricultural practices and modern industry. At present fresh water supplies are adequate to meet the demand in most areas of the country. However, if present trends continue, the need for fresh water will increase faster than the development of fresh water resources.[1]

Surface water and ground water comprise the two main forms of fresh water. To date the greatest emphasis has been placed on the development of surface water reserves although much larger quantities of fresh water are present in the form of ground water.

In glaciated areas, water may be present in sand and gravel deposits. These ground water supplies, called aquifers, are often of useable quality and the water can be extracted by conventional pumping techniques. The development of these ground water supplies has progressed slowly since traditional mapping techniques are expensive and time consuming. A mapping method presently used involves the drilling of a series of test wells. Since this process is expensive and time consuming, detailed explorations have not been conducted in many areas.

---

[1] O. E. Meinzer in Ground Water and Wells, G. F. Briggs and A. F. Fiedler, Ed., (E. E. Johnson, Inc., St. Paul, Minn., 1966), Chapter 1.

A new geophysical exploration technique called thermal prospecting has recently been proposed.[2] This method is based on the much higher heat capacity of water-saturated material compared to a similar dry material. Water-saturated material in the form of an aquifer will act as a heat sink in the summer and as a heat source in the winter. This heat sink or source will cause the soil temperature above the aquifer to be cooler in the summer and warmer in the winter than the soil temperature to be expected if no aquifer were present. This temperature deviation is called a thermal anomaly.

Thermal anomalies have been measured at a depth of 50 cm for several different locations of known aquifers.[3] The maximum thermal anomaly observed at each site varied from 1°C to 3°C.

Myers has reported detecting thermal patterns on the land surface using air-borne thermal remote sensors.[4] Correlations of the temperature differences with the presence of known aquifers have been made and the results indicate that the cooler regions can be associated with the presence of an aquifer. The surface thermal patterns, however, can not be detected under all conditions. Thus a tentative set of environmental conditions favorable to the detection of thermal

---

[2] K. Cartwright, Illinois State Geological Survey Circular 433, Urbana, Illinois, 1968.

[3] Ibid., pp. 19-38.

[4] V. I. Myers, NASA Report MSC-03742, Houston, Texas, Dec. 1970, Section 48.

patterns has been proposed on the basis of the data collected.[5] Since these conditions are based on a limited amount of data, no conclusive evidence has been presented.

The purpose of this study is to theoretically investigate the relationship between the surface thermal anomaly as detected by Myers and the subsurface anomaly as measured by Cartwright. Selected environmental factors will be varied to determine their effect on the magnitude of the surface thermal anomaly.

---

[5] D. G. Moore and V. I. Myers, RSI Report 72-06, Brookings, So. Dak., Feb. 1972.

CHAPTER 2. REVIEW OF BASIC CONCEPTS

Transfer of Heat in Soils

Heat can be transferred in soils by conduction, mass transfer of water, condensation and evaporation of water, and convection. In dry soils the primary heat transfer mechanism is conduction. In a wet soil, the movement of water in the soil can also be significant in the transfer of heat. Moisture can also evaporate in one region, diffuse to another region, and then condense resulting in the transfer of heat. Finally, the movement of air in the soil can transfer heat from one region to another.

The combined mathematical treatment of all four mechanisms is extremely difficult. A good approximation can be made, however, by combining all four mechanisms into a single equivalent mechanism similar to conduction.[6] The treatment of heat transfer in the soil may be mathematically treated as a conduction heat transfer problem. This will be the method used in the investigation of the problems considered.

The transfer of heat in a soil is determined by the composition of the soil and the temperature distribution within the soil. For one-dimensional heat transfer the quantity of heat transferred through a unit surface area per unit time is mathematically expressed as

$$q = -k\frac{\partial T}{\partial x} \qquad (2\text{-}1)$$

---

[6] D. A. deVries in Physics of Plant Environment, W. R. vanWijk, Ed., (North-Holland Publishing Co., Amsterdam, 1963), pp. 210-235.

where k is the thermal conductivity and $\frac{\partial T}{\partial x}$ is the thermal gradient describing the rate at which the temperature changes with depth. The thermal conductivity (k) depends on the properties of the soil. Equation (2-1) is valid only for a homogeneous material and cannot be strictly applied to a soil since it is a composite material. The equation can still be used, though, by determining an average conductivity for the soil on a macroscopic basis.[7]

A volume of soil material will increase in temperature if the heat flux into the volume is greater than the heat flux out of the volume provided no phase change of water occurs. The volumetric heat capacity (ρc) of a soil is the amount of heat needed to raise the temperature of a unit volume of soil material one degree, where ρ is the density of the soil and c is the gravimetric heat capacity.

The rate at which the temperature of a volume of soil material increases is dependent on the conductivity and the heat capacity of the soil. The thermal diffusivity expresses this rate of temperature increase and is defined as

$$\alpha = \frac{k}{\rho c} . \qquad (2\text{-}2)$$

Another important heat transfer equation is obtained from the law of conservation of energy. This law requires that the energy entering a unit volume of soil material must either leave the volume or cause

---

[7] Ibid.

the temperature of the soil to increase. Application of this law results in the second-order partial differential equation

$$\frac{\partial^2 T}{\partial x^2} = \frac{1}{\alpha} \frac{\partial T}{\partial t} . \qquad (2\text{-}3)$$

Equation (2-3) is called the governing equation.[8] This equation must be solved subject to conditions specified by the heat transfer problem. For a one-dimensional heat transfer problem these conditions consist of an initial condition and boundary conditions. The initial condition specifies the temperature distribution within the soil initially.

Boundary conditions can be separated into the following three groups:[9]

1. Boundary condition of the first kind. This type of condition specifies the temperature at the boundary. It has the form

$$T(a,t) = f(a,t) \qquad (2\text{-}4)$$

where a is the coordinate of the boundary and f(a,t) is a specified function.

2. Boundary condition of the second kind. This type of condition specifies the magnitude of the heat flux at the boundary and may be written as

$$\frac{\partial T}{\partial X} \Big|_{x=a} = f(a,t) . \qquad (2\text{-}5)$$

---

[8] D. Kirkham and W. L. Powers, Advanced Soil Physics, (John Wiley and Sons, Inc., New York, 1972), pp. 462-490.

[9] M. N. Özisik, Boundary Value Problems of Heat Conduction, (International Textbook Co., Scranton, 1968), pp. 7-9.

3. Boundary condition of the third kind. This type of condition is a linear combination of the first two conditions. It may be written as

$$k \left.\frac{\partial T}{\partial x}\right|_{x=a} + hT(a,t) = f(a,t) \qquad (2\text{-}6)$$

where k and h are coefficients specified by the boundary.

The above boundary conditions are homogeneous if $f(a,t) = 0$. Often a transformation may be performed to make the nonhomogeneous boundary conditions homogeneous. This may simplify the solution of the problem.

Energy Budget

Variations in soil temperature near the soil surface are primarily the result of periodic variations in the net radiation incident on the surface. The net radiation is the incoming solar, sky and atmospheric radiation minus the radiation reflected and emitted from the land surface. The law of conservation of energy can be used to write an energy budget equation expressing the exchange of heat at the land surface. The energy budget equation may be written as

$$S + B + L + V = 0 \qquad (2\text{-}7)$$

where S is the net radiation, B is the soil heat flow, L is the heat exchanged by conduction and mass movement of the air, and V is the heat used for the change of phase of water. Energy exchange may also occur

due to advection and precipitation. These terms have been omitted since they constitute a deviation from the normal situation.[10]

The energy budget equation can also be used if a plant canopy is present. The presence of a plant canopy may alter each individual term but the form of the energy balance equation will remain unchanged.

An example of the variation with time of each term in the energy budget equation is shown in Fig. 2-1. The positive direction of heat flow has been chosen towards the land surface. Notice that each term has the general form of a rectified sine wave. The main contributor to the energy balance is the radiation term. The other terms appear to be related to the radiation term and thus are in phase with it. Furthermore, the combined effect of S, L, and V can be approximately represented by the positive portion of a sine wave.

The net energy exchange on a calm clear night is primarily due to the effective outgoing radiation. Several empirical formulas have been developed to describe this term. The most well known of these equations are those by Ångström and Brunt.[11]

Ångström's equation is of the form

$$R = (A - B10^{-\gamma e})\,\sigma T^4 \qquad (2\text{-}8)$$

where R is the net radiation, A, B, and γ are empirical constants, e is the vapor pressure, σ is the Stefan-Boltzmann constant, and T is

---

[10] R. Geiger, The Climate Near the Ground, (Harvard University Press, Cambridge, 1955), pp. 5-43.

[11] O. G. Sutton, Micrometeorology, (McGraw-Hill Book Co., New York, 1953), pp. 174-181.

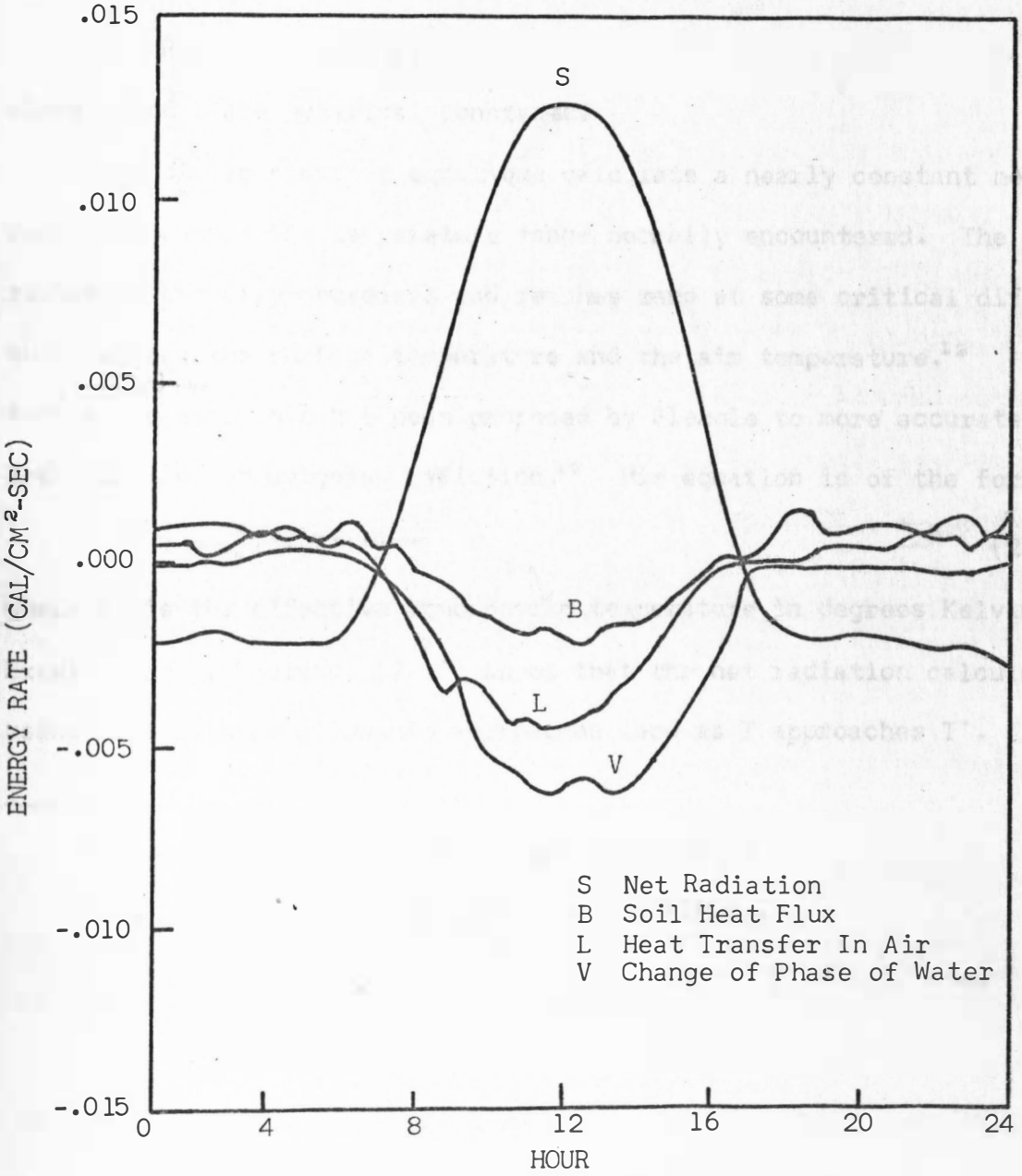

Fig. 2-1. Daily Variation in Heat Budget Terms for Alfalfa-Brome Grass at Handcock, Wisconsin September 27, 1957.*

*W. D. Sellers, Physical Climatology, (University of Chicago Press, Chicago, 1965), p. 112.

the surface temperature in degrees Kelvin. Brunt's equation if of the form

$$R = (a + b\sqrt{e})\,\sigma T^4 \qquad (2\text{-}9)$$

where a and b are empirical constants.

Both of the previous equations calculate a nearly constant net radiation within the temperature range normally encountered. The net radiation actually decreases and reaches zero at some critical difference between the surface temperature and the air temperature.[12] Another relationship has been proposed by Fleagle to more accurately describe the net outgoing radiation.[13] His equation is of the form

$$R = \sigma[T^4 - (T')^4] \qquad (2\text{-}10)$$

where T' is the effective atmospheric temperature in degrees Kelvin. Examination of Equation (2-10) shows that the net radiation calculated using Fleagle's relationship approaches zero as T approaches T'.

---

[12] H. Wexler, Mon. Wea. Rev., 64, 122 (1936).

[13] R. G. Fleagle, J. Meteorol., 7, 114 (1950).

CHAPTER 3. SIMULATION OF NOCTURNAL SOIL TEMPERATURES

Development of the Boundary Value Problem

One-dimensional heat transfer will be considered in two homogeneous soil layers extending from the surface $x = 0$ to a depth $x = L$. The value of L will be chosen as 50 cm since the daily soil temperature fluctuations become small at this depth.[14,15] Therefore, the lower boundary temperature of each soil layer will be assumed constant. Also, the lower boundary temperature of one soil layer (layer A) will be assumed to differ from the lower boundary temperature of the other layer (layer B) by an amount ΔT. The temperature difference ΔT corresponds to a thermal anomaly similar to an anomaly as measured by Cartwright.[16]

The upper surface temperature of both layers will be assumed to be initially identical. Furthermore, the initial temperature profiles of the two soil layers will be assumed to differ by a depth-dependent term $\phi(x)\Delta T$, where $\phi(0) = 0$ and $\phi(L) = 1$. Both profiles will also be assumed to be dissipating heat from the soil surface $x = 0$ at a constant and equal rate q. Figure 3-1, called a tautochrone, shows the vertical temperature profile for soil layer A. Figure 3-2 shows the tautochrone for soil layer B.

---

[14] J. E. Carson, Technical Report ANL-6470, Argonne, Ill., Nov. 1961, p. 31.

[15] K. Cartwright, op. cit., pp. 19-20.

[16] Ibid., pp. 19-38.

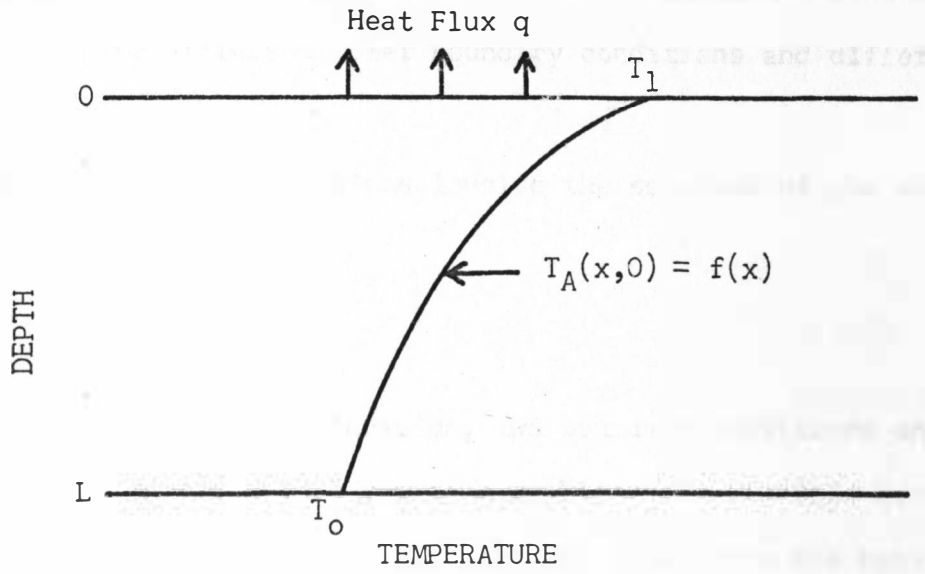

Fig. 3-1. Tautochrone for Soil Layer A.

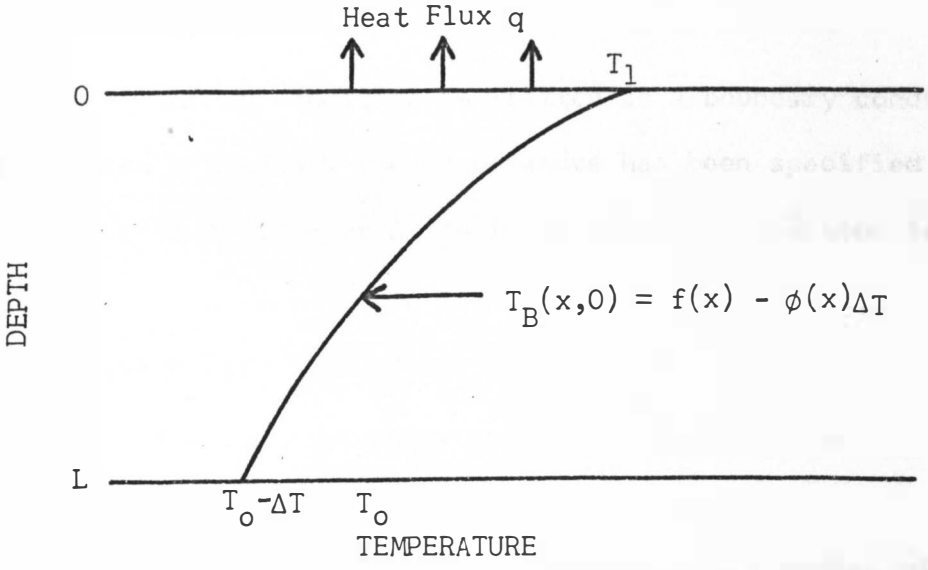

Fig. 3-2. Tautochrone for Soil Layer B.

Two transient heat transfer problems must be solved since the two soil layers have different lower boundary conditions and different initial conditions.

Both heat transfer problems involve the solution of the second order differential equation

$$\frac{\partial^2 T}{\partial x^2} = \frac{1}{\alpha} \frac{\partial T}{\partial t} . \tag{3-1}$$

To solve this differential equation, two boundary conditions and one initial condition are needed for each problem. The surface boundary condition at $x = 0$ is identical for both problems since the heat flux is assumed to be identical for both soil layers. The upper boundary condition for both soil layers is written as a boundary condition of the second kind. Thus

$$q = k \frac{\partial T(0,t)}{\partial x} . \tag{3-2}$$

The lower boundary condition is written as a boundary condition of the first kind since only the temperature has been specified for this boundary. For soil layer A the lower boundary condition is written as

$$T_A(L,t) = T_o. \tag{3-3}$$

For soil layer B the lower boundary condition is written as

$$T_B(L,t) = T_o - \Delta T. \tag{3-4}$$

The initial temperature profile is written as a function of the depth within the soil layer. For soil layer A the initial condition is written as

$$T_A(x,0) = f(x). \tag{3-5}$$

It has previously been assumed that the initial temperature profiles differ by a function $\phi(x)\,\Delta T$. Thus, the initial temperature profile for soil layer B is written as

$$T_B(x,0) = f(x) - \phi(x)\,\Delta T. \tag{3-6}$$

A finite-integral transform will be used to solve the two heat transfer problems previously defined. Lumsdaine indicates that the solution obtained by a finite-integral transform will converge more rapidly if the nonhomogeneous boundary conditions are made homogeneous.[17] The boundary conditions will, therefore, be made homogeneous.

The nonhomogeneous boundary conditions for soil layer A are made homogeneous by letting

$$T_A(x,t) = V_A(x,t) + (x-L)\,\frac{q}{k} + T_o. \tag{3-7}$$

Substituting Eq. (3-7) into the governing equation given by Eq. (3-1) results in the new governing equation for soil layer A

$$\frac{\partial^2 V_A}{\partial x^2} = \frac{1}{\alpha}\,\frac{\partial V_A}{\partial t}. \tag{3-8}$$

The two boundary conditions given by Eq. (3-2) and Eq. (3-3) are transformed into the homogeneous boundary conditions

$$k\,\frac{\partial V_A(0,t)}{\partial x} = 0 \tag{3-9a}$$

$$V_A(L,t) = 0. \tag{3-9b}$$

---

[17] E. Lumsdaine, Engr. Exp. Sta. Bull. 17, Brookings, So. Dak., Nov. 1970.

The initial condition for soil layer A given by Eq. (3-5) is transformed into the new initial condition

$$V_A(x,0) = f(x) - (x-L)\frac{q}{k} - T_o. \tag{3-9c}$$

A slightly different substitution is required to make the non-homogeneous boundary condition for soil layer B homogeneous. For soil layer B let

$$T_B(x,t) = V_B(x,t) + (x-L)\frac{q}{k} + T_o - \Delta T. \tag{3-10}$$

Substituting Eq. (3-10) into the governing equation given by Eq. (3-1) results in the new governing equation

$$\frac{\partial^2 V_B}{\partial x^2} = \frac{1}{\alpha}\frac{\partial V_B}{\partial t}. \tag{3-11}$$

The new boundary conditions for soil layer B are obtained by substituting Eq. (3-10) into Eqs. (3-2) and (3-4). The new boundary conditions become

$$k\frac{\partial V_B(0,t)}{\partial x} = 0 \tag{3-12a}$$

$$V_B(L,t) = 0. \tag{3-12b}$$

Likewise, the initial condition for soil layer B given by Eq. (3-6) becomes the new initial condition

$$V_B(x,0) = f(x) - (x-L)\frac{q}{k} - T_o + \Delta T\,[1-\phi(x)]. \tag{3-12c}$$

The form of Eq. (3-9c) and Eq. (3-12c) may be simplified by defining the functions

$$Z_A(x) \equiv f(x) - (x-L)\frac{q}{k} - T_o \tag{3-13a}$$

$$Z_B(x) \equiv f(x) - (x-L)\frac{q}{k} - T_o + \Delta T\,[1-\phi(x)]. \tag{3-13b}$$

The initial conditions for the two soil layers then become

$$V_A(x,0) = Z_A(x) \tag{3-14a}$$

$$V_B(x,0) = Z_B(x). \tag{3-14b}$$

Comparison of Eq. (3-8) and Eq. (3-11) shows that the form of the governing equation for both problems is identical. Comparing Eqs. (3-9a), (3-9b), and (3-14a) with Eqs. (3-12a), (3-12b), and (3-14b) shows that the forms of the boundary conditions and initial condition are also identical for both problems. The substitutions which have been performed have, therefore, reduced the two problems to a single general problem. The governing equation for the general problem is

$$\frac{\partial^2 V}{\partial x^2} = \frac{1}{\alpha}\frac{\partial V}{\partial t} \tag{3-15}$$

subject to the boundary conditions

$$k\,\frac{\partial V(0,t)}{\partial x} = 0 \tag{3-16a}$$

$$V(L,t) = 0 \tag{3-16b}$$

and the initial condition

$$V(x,0) = Z(x). \tag{3-16c}$$

Solution of Boundary Value Problem by Finite-Integral Method

The important fundamental concepts of the finite-integral transform method will now be discussed and used to solve the previously defined boundary value problem. A more detailed discussion of the theory and use of a finite-integral transform may be found in the book by Koshlyakov, Smirnov, and Gliner.[18]

Consider the application of a finite-integral transform to a partial differential equation of the form

$$MV + M'V = f \tag{3-17}$$

where V is the unknown function, f is a known function of the variables, M'V contains no derivatives with respect to the variable of transformation, and

$$MV = a\frac{\partial^2 V}{\partial x^2} + b\frac{\partial V}{\partial x} + g\,V. \tag{3-18}$$

Comparison of Eq. (3-15) with Eq. (3-17) yields

$$MV = \frac{\partial^2 V}{\partial x^2} \tag{3-19a}$$

$$M'V = -\frac{1}{\alpha}\frac{\partial V}{\partial t} \tag{3-19b}$$

$$f = 0. \tag{3-19c}$$

---

[18] N. S. Koshlyakov, M. M. Smirnov, and E. B. Gliner, Differential Equations of Mathematical Physics, (North-Holland Publishing Co., Amsterdam, 1964), pp. 521-562.

Equation (3-19a) requires the coefficients in Eq. (3-18) to have the values

$$a = 1 \qquad b = 0 \qquad g = 0. \tag{3-20}$$

The finite-integral transform is defined by the relationship

$$\bar{V} = \int_0^L VK(x, \gamma)dx \tag{3-21}$$

where $K(x, \gamma)$ is called the kernel of the transform and γ is the transformed variable. The limits of integration in the previous equation coincide with the limits of variation of the variable of transformation. The variable of transformation in this problem varies from $x = 0$ to $x = L$.

The transformed relationship will contain no integral terms if the kernel satisfies the equation

$$\frac{\partial^2 aK}{\partial x^2} - \frac{\partial bK}{\partial x} + g K = - \lambda^2 K \tag{3-22}$$

where λ does not depend on the variable of transformation.[19]

A normalized kernel $\bar{K}(x, \gamma)$ may be defined by the relationship

$$K(x, \gamma) = \frac{1}{C_\gamma} \rho(x)\bar{K}(x, \gamma) \tag{3-23}$$

where C_γ is a normalizing divisor and $\rho(x)$ is a function to be determined. Substituting Eq. (3-23) into Eq. (3-22) yields the relationship for the normalized kernel

$$a\rho \frac{\partial^2 \bar{K}}{\partial x^2} + \left(2 \frac{da\rho}{dx} - b\rho\right) \frac{\partial \bar{K}}{\partial x} - \delta \bar{K} = - \lambda^2 \rho \bar{K} \tag{3-24}$$

---

[19] Ibid., pp. 522-525.

where

$$\delta \equiv -\left(\frac{d^2 a\rho}{dx^2} - \frac{db\rho}{dx} + g\rho\right). \tag{3-25}$$

Provided the function $\rho(x)$ satisfies the differential equation

$$\frac{da\rho}{dx} = b\rho\,, \tag{3-26}$$

Eq. (3-24) can be written in the form of the Sturm-Liouville problem

$$\frac{\partial}{\partial x}\left(p\,\frac{\partial \bar{K}}{\partial x}\right) - \delta\bar{K} + \lambda^2\rho\bar{K} = 0 \tag{3-27}$$

where

$$p = a\rho \quad , \quad \delta = -g\rho\,. \tag{3-28}$$

Taking the derivative of the product $a\rho$ in Eq. (3-26) results in the differential equation

$$a\,\frac{d\rho}{dx} + \left(\frac{da}{dx} - b\right)\rho = 0. \tag{3-29}$$

The solution of this differential equation is

$$\rho(x) = \exp\left[-\int_0^L \frac{1}{a}\left(\frac{da}{dx} - b\right)dx\right]. \tag{3-30}$$

The coefficients a and b were previously determined and are given by Eq. (3-20). The coefficients in the Sturm-Liouville problem are obtained by solving Eq. (3-30). Using the results obtained in Eqs. (3-30) and (3-28), Eq. (3-27) becomes

$$\frac{\partial^2 \bar{K}}{\partial x^2} + \lambda^2\bar{K} = 0 \tag{3-31}$$

which is the differential equation to be satisfied by the normalized kernel $\bar{K}$.

A set of homogeneous boundary conditions can be selected for the normalized kernel of a form identical to the boundary conditions of the original problem.[20] From the original boundary conditions given by Eqs. (3-16a) and (3-16b), the boundary conditions for the normalized kernel become

$$\frac{\partial \bar{K}(0)}{\partial x} = 0 \tag{3-32a}$$

$$\bar{K}(L) = 0 . \tag{3-32b}$$

The general solution of Eq. (3-31) is of the form

$$\bar{K}(x) = A \sin \lambda x + B \cos \lambda x. \tag{3-33}$$

The first boundary condition given by Eq. (3-32a) requires that

$$A = 0 . \tag{3-34}$$

The second boundary condition given by Eq. (3-32a) also requires that

$$\bar{K}(L) = \cos \lambda L = 0 . \tag{3-35}$$

The roots of the previous equation are

$$\lambda_\gamma = \frac{(2\gamma-1)\pi}{2L} \qquad \gamma = 1,2\cdots. \tag{3-36}$$

The normalized kernel given by Eq. (3-33) subject to Eqs. (3-34), (3-35), and (3-36) thus becomes

$$\bar{K}(x) = \cos \lambda_\gamma x \qquad \gamma = 1,2,\cdots. \tag{3-37}$$

---

[20] Ibid., pp. 528-530.

To determine the transform kernel K, the normalizing divisor C_γ must be determined. The normalizing divisor can be determined by the relationship[21]

$$C_\gamma = \int_0^L \rho(x)\, \overline{K}^2(x)dx. \tag{3-38}$$

The transform kernel is obtained by substituting the results obtained from Eqs. (3-30) and (3-38) into Eq. (3-23). The result is

$$K(x) = \frac{2}{L} \cos \lambda_\gamma x. \tag{3-39}$$

The finite-integral transform may now be performed since the transform kernel has been determined for the problem. The integral transform is performed by multiplying the governing equation given by Eq. (3-15) by the transform kernel and integrating over the interval of variation. Thus

$$\int_0^L \frac{\partial^2 V}{\partial x^2} K(x)dx = \frac{1}{\alpha} \int_0^L \frac{\partial V}{\partial t} K(x)dx. \tag{3-40}$$

Integrating by parts, using the previously determined boundary conditions together with Eq. (3-22), one can show that

$$\int_0^L \frac{\partial^2 V}{\partial x^2} K(x)dx = - \int_0^L \lambda_\gamma^2 V K(x)dx. \tag{3-41}$$

Eq. (3-40) can then be written as

$$\int_0^L \lambda_\gamma^2 V K(x)dx = -\frac{1}{\alpha} \int_0^L \frac{\partial V}{\partial t} K(x)dx. \tag{3-42}$$

---

[21] Ibid., pp. 527-530.

From the definition of the integral transform, the previous equation becomes

$$- \lambda^2_\gamma \, \bar{V} = \frac{1}{\alpha} \frac{d\bar{V}}{dt} \cdot \tag{3-43}$$

The partial derivative in Eq. (3-42) has become a total derivative since the variable x has been integrated over definite limits. The solution of Eq. (3-43) is

$$\bar{V}(t) = \bar{V}(0) e^{-\alpha \lambda_\gamma^2 t} \tag{3-44}$$

where $\bar{V}(0)$ is the transformed initial condition.

From the results of the Sturm-Liouville problem, the inverse for the transformed function is[22]

$$V(x,t) = \sum_{\gamma=1}^{\infty} \bar{V}(t) \, \bar{K}(x). \tag{3-45}$$

Using Eqs. (3-37) and (3-44), the function V(x,t) becomes

$$V(x,t) = \sum_{\gamma=1}^{\infty} \bar{V}(0) e^{-\alpha \lambda_\gamma^2 t} \cos \lambda_\gamma x. \tag{3-46}$$

The transformed initial condition $\bar{V}(0)$ is obtained by multiplying the initial condition given by Eq. (3-16c) by the transform kernel and integrating over the range of the variable of transformation. Thus

$$\bar{V}(0) = \frac{2}{L} \int_0^L Z(x) \cos \lambda_\gamma x \, dx \tag{3-47}$$

where Z(x) is the initial condition for the general problem.

---

[22] Ibid.

Substitution of Eq. (3-47) into Eq. (3-46) finally yields

$$V(x,t) = \frac{2}{L} \sum_{\gamma=1}^{\infty} e^{-\alpha \lambda_\gamma^2 t} \cos \lambda_\gamma x \int_0^L Z(x) \cos \lambda_\gamma x \, dx. \qquad (3\text{-}48)$$

The function $V(x,t)$ was obtained from the original temperature function $T_A(x,t)$ for soil layer A by using Eq. (3-7). Substituting Eq. (3-48) into Eq. (3-7) yields for the temperature of soil layer A

$$T_A(x,t) = T_o + (x-L)\frac{q}{k} + \frac{2}{L} \sum_{\gamma=1}^{\infty} e^{-\alpha \lambda_\gamma^2 t} \cos \lambda_\gamma x$$

$$\int_0^L Z_A(x) \cos \lambda_\gamma x \, dx. \qquad (3\text{-}49)$$

Similarily, Eq. (3-10) transformed the original temperature function $T_B(x,t)$ for soil layer B into the same general function $V(x,t)$. Substituting Eq. (3-48) into Eq. (3-10) yields for the temperature of soil layer B

$$T_B(x,t) = T_o + (x-L)\frac{q}{k} - \Delta T + \frac{2}{L} \sum_{\gamma=1}^{\infty} e^{-\alpha \lambda_\gamma^2 t} \cos \lambda_\gamma x$$

$$\int_0^L Z_B(x) \cos \lambda_\gamma x \, dx. \qquad (3\text{-}50)$$

Now the functions $Z_A(x)$ and $Z_B(x)$ were defined by Eqs. (3-13a) and (3-13b). Comparison of these two equations shows that the functions are interrelated by the relationship

$$Z_B(x) = Z_A(x) + \Delta T \, [1 - \phi(x)]. \qquad (3\text{-}51)$$

Substitution into Eq. (3-50) yields for soil layer B

$$T_B(x,t) = T_o + (x-L)\frac{q}{k} - \Delta T + \frac{2}{L}\sum_{\gamma=1}^{\infty} e^{-\alpha \lambda_\gamma^2 t} \cos \lambda_\gamma x$$

$$\left\{\int_o^L Z_A(x) \cos \lambda_\gamma x \, dx + \Delta T \int_o^L [1-\phi(x)] \cos \lambda_\gamma x \, dx\right\}. \qquad (3\text{-}52)$$

The magnitude of the thermal anomaly at any depth may be obtained by subtracting Eq. (3-52) from Eq. (3-49). Thus

$$T_A(x,t) - T_B(x,t) = \Delta T - \frac{2\Delta T}{L}\sum_{\gamma=1}^{\infty} e^{-\alpha \lambda_\gamma^2 t} \cos \lambda_\gamma x$$

$$\int_o^L [1-\phi(x)] \cos \lambda_\gamma x \, dx \qquad (3\text{-}53)$$

or for the surface thermal anomaly at $x = 0$

$$T_A(0,t) - T_B(0,t) = \Delta T - \frac{2\Delta T}{L}\sum_{\gamma=1}^{\infty} e^{-\alpha \lambda_\gamma^2 t}$$

$$\int_o^L [1-\phi(x)] \cos \lambda_\gamma x \, dx. \qquad (3\text{-}54)$$

The previous equation shows that the surface thermal anomaly is dependent on the thermal diffusivity (α), the magnitude of the thermal anomaly at 50 cm (ΔT), and the form of the initial temperature difference between soil profiles (ϕ). Note also that the form of the initial temperature profile and the surface heat flux does not appear in Eq. (3-54).

Analysis of Analytic Solution

Consider the effect the form of $\phi(x)$ has on the development of a surface thermal anomaly. Let

$$\phi(x) = \frac{x}{L} . \tag{3-55}$$

Evaluation of the integral term in Eq. (3-54) yields

$$\int_0^L [1 - \frac{x}{L}] \cos \lambda_\gamma x \, dx = \frac{1}{L\lambda_\gamma^2} . \tag{3-56}$$

Equation (3-54) then becomes

$$T_A(0,t) - T_B(0,t) = \Delta T - \frac{2\Delta T}{L^2} \sum_{\gamma=1}^{\infty} \frac{e^{-\alpha\lambda_\gamma^2 t}}{\lambda_\gamma^2} . \tag{3-57}$$

The magnitude of the surface thermal anomaly may now be calculated by selecting a value for the thermal diffusivity (α). Unless otherwise stated, representative values for the thermal properties used in all subsequent calculations are:

$$\text{Thermal conductivity } (k) = 0.0036 \frac{\text{cal}}{\text{cm-sec-}^\circ\text{C}}$$

$$\text{Heat capacity } (\rho c) = 0.5000 \frac{\text{cal}}{\text{cm}^3\text{-}^\circ\text{C}}$$

$$\text{Thermal diffusivity } (\alpha) = 0.0072 \frac{\text{cm}^2}{\text{sec}} .$$

These values are for a clay soil with 20 volume percent water.[23]

---

[23] R. Geiger, op. cit., p. 171.

The results of a computer evaluation of Eq. (3-57) are contained in Table 3-1. Examination of this table shows that a significant thermal anomaly is developed in a few hours.

Now let the function

$$\phi(x) = \frac{x^2}{L^2} \tag{3-58}$$

The integral term in Eq. (3-54) then becomes

$$\int_0^L [1 - \frac{x^2}{L^2}] \cos \lambda_\gamma x \, dx = \frac{(-1)^{\gamma-1}}{L^2 \lambda_\gamma^3} . \tag{3-59}$$

Substitution into Eq. (3-54) now yields the surface anomaly given as

$$T_A(0,t) - T_B(0,t) = \Delta T - \frac{2\Delta T}{L^3} \sum_{\gamma=1}^{\infty} \frac{(-1)^{\gamma-1}}{\lambda_\gamma^3} e^{-\alpha \lambda_\gamma^2 t} . \tag{3-60}$$

The results of a computer evaluation of Eq. (3-60) are shown in Table 3-2. Comparing Table 3-2 with Table 3-1 shows that the surface thermal anomaly using the quadradic form of $\phi(x)$ given by Eq. (3-58) is one half as large as the anomaly obtained using the linear form given by Eq. (3-55). Even though the surface temperatures are very similar, the surface thermal anomaly developed is much different in magnitude for the different forms of $\phi(x)$.

The development of a surface thermal anomaly for a quadradic and a linear form of $\phi(x)$ is also shown in Fig. 3-3. The surface thermal anomalies shown in Fig. 3-3 can also be seen to develop differently with time. Therefore, the selection of a form for $\phi(x)$ appears significant in the study of the development of a surface thermal anomaly.

Table 3-1: Development of a Surface Thermal Anomaly With Time for a Linear Difference Between Initial Temperature Profiles.

Elapsed Time (hrs.)	Surface Temperature of Profile A (°C)	Surface Temperature of Profile B (°C)	Percent of the Subsurface Thermal Anomaly Developed on the Surface
0	26.916	26.912	0.4
1	24.685	24.570	11.5
2	23.755	23.592	16.2
3	23.051	22.852	19.9
4	22.463	22.233	23.0
5	21.949	21.692	25.7
6	21.488	21.206	28.1
7	21.065	20.761	30.4
8	20.674	20.349	32.5
9	20.308	19.963	34.5

Table 3-2: Development of a Surface Thermal Anomaly With Time for a Quadradic Difference Between Initial Temperature Profiles.

Elapsed Time (hrs.)	Surface Temperature of Profile A (°C)	Surface Temperature of Profile B (°C)	Percent of the Subsurface Thermal Anomaly Developed on the Surface
0	26.916	26.916	0.0
1	24.685	24.664	2.1
2	23.755	23.713	4.1
3	23.051	22.989	6.2
4	22.463	22.380	8.3
5	21.949	21.846	10.4
6	21.488	21.363	12.4
7	21.065	20.921	14.5
8	20.674	20.509	16.5
9	20.308	20.123	18.5

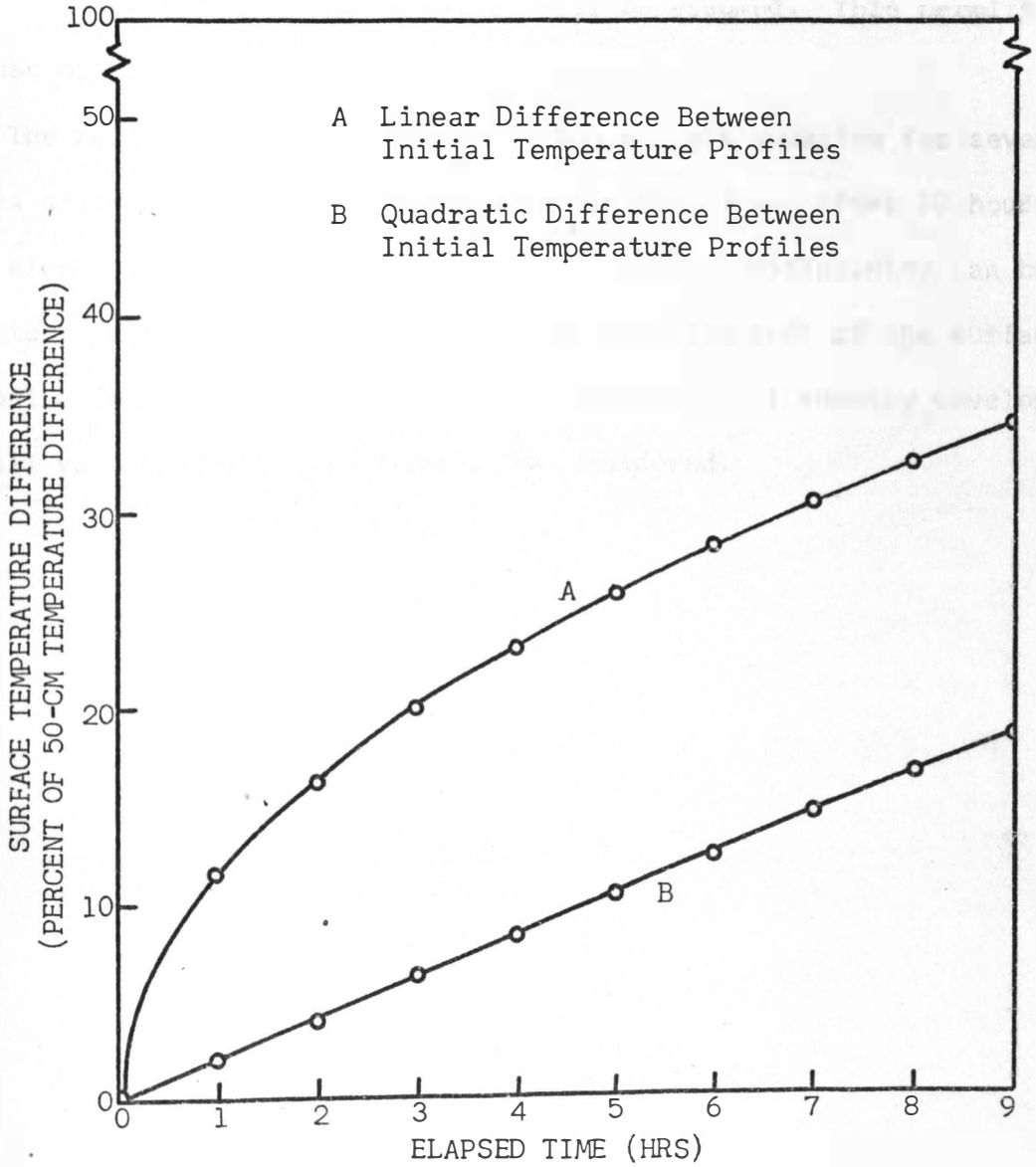

Fig. 3-3. Development of a Surface Thermal Anomaly With Time for Two Different Forms of the Depth Dependent Difference Between Initial Temperature Profiles.

The surface thermal anomaly also appears to be dependent on the thermal diffusivity of the soil. To study the influence this factor has on the development of a surface thermal anomaly, a linear difference in initial temperature profiles will be assumed. This permits the use of Eq. (3-57).

The results of a computer evaluation of this equation for several values of thermal diffusivity are shown in Fig. 3-4. After 10 hours have elapsed, a five-fold increase in the thermal diffusivity can be seen to result in a two-fold increase in the magnitude of the surface thermal anomaly. Furthermore, a significant thermal anomaly develops for all values of thermal diffusivity considered.

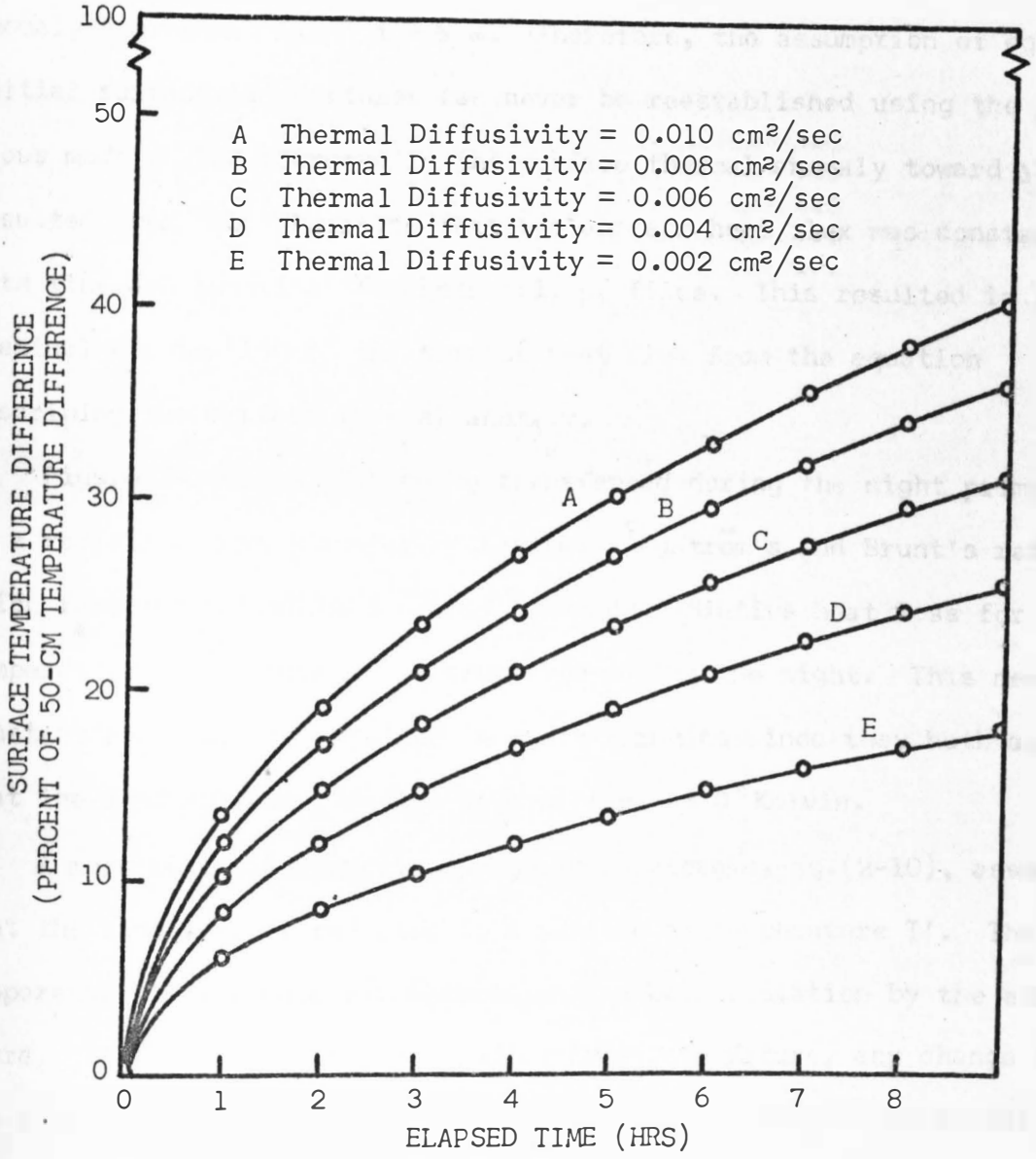

Fig. 3-4. Development of a Surface Thermal Anomaly With Time for Different Values of Thermal Diffusivity.

CHAPTER 4. SIMULATION OF DIURNAL SOIL TEMPERATURES

The surface thermal anomaly shown in Fig. 3-3 increases with the elapsed time. Equation (3-54) also shows that the surface thermal anomaly approaches ΔT as $t \rightarrow \infty$. Therefore, the assumption of equal initial surface temperatures can never be reestablished using the previous model. The increase in the surface thermal anomaly toward ΔT resulted from the assumption that the surface heat flux was constant with time and identical for both soil profiles. This resulted in the eventual elimination of the surface heat flux from the equation describing the surface thermal anomaly.

Figure 2-1 shows heat being transferred during the night primarily by a radiative heat transfer mechanism. Ångström's and Brunt's radiation formulas calculate a nearly constant radiative heat loss for the temperature ranges normally encountered during the night. This nearly constant heat loss is obtained in their formulas since they both assume that the land surface radiates to a surface at 0°Kelvin.

A more realistic equation proposed by Fleagle, Eq.(2-10), assumes that the land surface radiates to a surface at temperature T'. The temperature T' accounts for absorption and back radiation by the atmosphere. If T' is close to the land surface temperature, any change in the surface temperature or T' will produce a much larger fractional change in the heat loss calculated as compared to the change calculated using Ångström's or Brunt's equation. Fleagle's radiation equation will therefore be used to consider the effect of a temperature dependent

heat loss term on the magnitude of the surface thermal anomaly developed. Since radiative boundary conditions are difficult to handle analytically, a finite-difference numerical technique will be used to solve the new heat transfer problem.

Development of Finite-Difference Model

An approximated derivative is used in the finite-difference method to solve differential equations. The theory of finite differences may be found in many heat transfer texts.[24-27]

The derivative of a function is defined as

$$\frac{du}{dx} = \lim_{\Delta x \to \infty} \frac{u(x + \Delta x) - u(x)}{\Delta x} . \qquad (4\text{-}1)$$

The finite-difference method assumes that a Δx may be chosen sufficiently small to permit the omission of the limit. Equation (4-1) then becomes

$$\frac{du}{dx} = \frac{u(x + \Delta x) - u(x)}{\Delta x} . \qquad (4\text{-}2)$$

---

[24] G. E. Myers, Analytical Methods in Conduction Heat Transfer, (McGraw-Hill Book Co., New York, 1971), pp. 233-315.

[25] M. N. Özisik, op. cit., pp. 388-425.

[26] G. M. Dusinberre, Heat-Transfer Calculations by Finite Differences, (International Textbook Co., Scranton, 1961).

[27] H. S. Carslaw and J. C. Jaeger, Conduction of Heat in Solids, 2nd ed., (Clarendon Press, Oxford, 1959), pp. 466-478.

Higher order derivatives may be similarly defined. Identical results may also be obtained by expanding the function u in a Taylor series about the point x.[28]

Consider now a slab of thickness L. Figure 4-1 shows the assignment of m equally spaced reference points to the slab. The m reference points are usually referred to as nodal points. Notice that nodal point 1 coincides with the upper surface of the slab at $x = 0$. The point m coincides with the other boundary at $x = L$. The distance between each nodal point is assumed to be an equal interval Δx. The heat flux into the surface $x = 0$ has been denoted q_S while the heat flux out of the lower surface at $x = L$ is denoted as q_L.

Now consider a volume of material surrounding node n ($n = 2,3,\cdots,m-1$) as shown in Fig. 4-2. The volume of the material surrounding node n is $A\Delta x$ where A is a unit surface area and Δx is the distance between nodal points. The amount of heat transferred from node $n-1$ to node n is denoted by $q_{n-1,n}$ and the amount of heat transferred from node n to node $n+1$ is denoted by $q_{n,n+1}$. The heat stored within the volume is given by $\dot{E}_{sn}$.

---

[28]M. N. Özisik, op. cit., pp. 391-396.

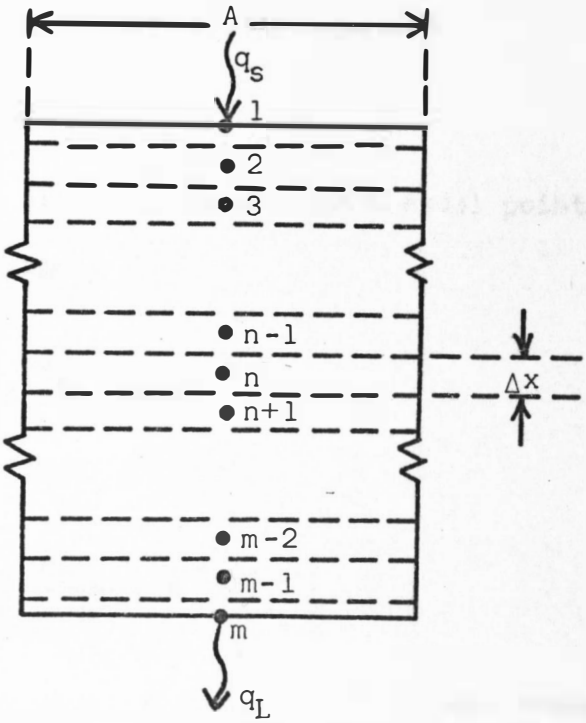

Fig. 4-1. Assignment of Nodal Points and Heat Flux Terms for the Finite-Difference Model.

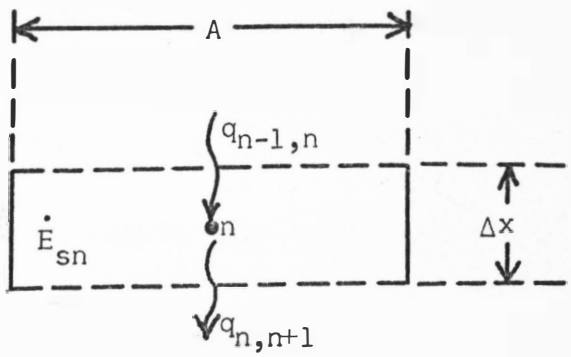

Fig. 4-2. Energy Balance for Node n.

For one dimensional heat transfer, the law of conservation of energy applied to node n results in the equation

$$q_{n-1,n} = q_{n,n+1} + \dot{E}_{sn}. \tag{4-3}$$

The rate at which heat is transferred between nodal points is written in finite-difference form as

$$q_{n-1,n} = - kA \frac{T_n - T_{n-1}}{\Delta x} \tag{4-4a}$$

$$q_{n,n+1} = - kA \frac{T_{n+1} - T_n}{\Delta x} \tag{4-4b}$$

where T_{n-1} is the temperature of node n-1, T_n is the temperature of node n, T_{n+1} is the temperature of node n+1, and k is the thermal conductivity of the material between the nodal points. If the conductivity of the volume element surrounding each nodal point is different, the conductivity between nodal points may be written as the average of the volume elements. Thus for Eq. (4-4a)

$$k = \frac{k_{n-1} + k_n}{2} . \tag{4-5}$$

Equation (4-4a) may then be written as

$$q_{n-1,n} = - \left(\frac{k_{n-1} + k_n}{2}\right) A \frac{T_n - T_{n-1}}{\Delta x} . \tag{4-6a}$$

Similarly, Eq. (4-4b) becomes

$$q_{n,n+1} = -\left(\frac{k_n + k_{n+1}}{2}\right)_A \frac{T_{n+1} - T_n}{\Delta x} . \qquad (4\text{-}6b)$$

The energy storage term expresses the rate at which the temperature of the volume changes. This term may be written in finite-difference form as

$$\dot{E}_{sn} = (\rho c)_n A \Delta x \frac{T_n' - T_n}{\Delta t} \qquad (4\text{-}7)$$

where Δt is the time increment, T_n is the temperature of node n at time t and T_n' is the temperature of node n at time $t+\Delta t$.

Substituting Eqs. (4-6a), (4-6b), and (4-7) into Eq. (4-3) and rearranging terms yields

$$\frac{T_n' - T_n}{\Delta t} = \frac{1}{2(\rho c)_n (\Delta x)^2}\left[(k_{n-1} + k_n)T_{n-1} - (k_{n-1} + 2k_n + k_{n+1})T_n + (k_n + k_{n+1})T_{n+1}\right]. \qquad (4\text{-}8)$$

Solving for the temperature at time $t+\Delta t$ results in the equation

$$T_n' = \frac{(k_{n-1} + k_n)\Delta t}{2(\rho c)_n (\Delta x)^2} T_{n-1} + \left[1 - \frac{(k_{n-1} + 2k_n + k_{n+1})\Delta t}{2(\rho c)_n (\Delta x)^2}\right]T_n + \frac{(k_n + k_{n+1})\Delta t}{2(\rho c)_n (\Delta x)^2} T_{n+1} . \qquad (4\text{-}9)$$

Now consider the transfer of heat at the surface x = 0. Figure 4-3 shows the volume element for node 1.

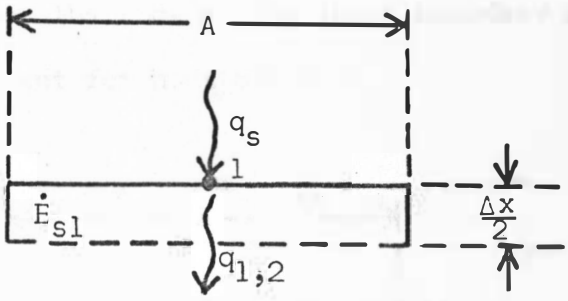

Fig. 4-3. Energy Balance for Node 1.

The energy balance can be written as

$$q_s = q_{1,2} + \dot{E}_{s1}. \tag{4-10}$$

The rate of heat transfer from node 1 to node 2 is

$$q_{1,2} = -\left(\frac{k_1 + k_2}{2}\right) A \frac{T_2 - T_1}{\Delta x}. \tag{4-11}$$

Now since node 1 is at the surface, the volume of material surrounding node 1 is $\frac{\Delta x}{2} A$. The energy storage term is then

$$\dot{E}_{s1} = (\rho c)_1 A \frac{\Delta x}{2} \frac{T_1' - T_1}{\Delta t}. \tag{4-12}$$

Substituting Eqs. (4-11) and (4-12) into Eq. (4-10) and rearranging yields

$$\frac{T_1' - T_1}{\Delta t} = \frac{2q_s}{A(\rho c)_1 \Delta x} + \frac{k_1 + k_2}{(\rho c)_1 (\Delta x)^2} [T_2 - T_1]. \tag{4-13}$$

Solving for the new temperature T_1' gives

$$T_1' = \frac{2q_s\Delta t}{A(\rho c)_1\Delta x} + \left[1 - \frac{(k_1 + k_2)\Delta t}{(\rho c)_1(\Delta x)^2}\right]T_1 + \frac{(k_1 + k_2)\Delta t}{(\rho c)_1(\Delta x)^2} T_2. \quad (4\text{-}14)$$

Finally, consider the node at the lower boundary $x = L$. Figure 4-4 shows the volume element for node m.

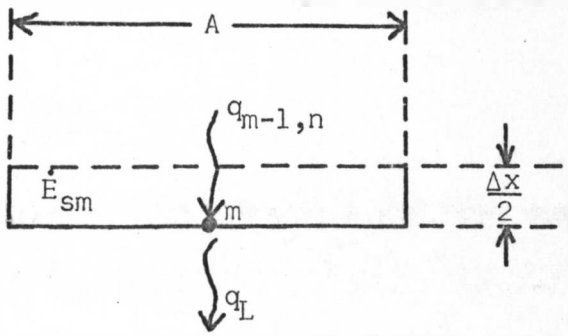

Fig. 4-4. Energy Balance for Node m.

The energy balance equation for node m is

$$q_{m-1,m} = q_L + \dot{E}_{sm}. \quad (4\text{-}15)$$

The rate of heat transfer from node m-1 to node m is

$$q_{m-1,m} = -\left(\frac{k_{m-1} + k_m}{2}\right) A \frac{T_m - T_{m-1}}{\Delta x}. \quad (4\text{-}16)$$

Again since the volume element surrounding node m is only $\frac{\Delta x}{2}$ A, the energy storage term can be written as

$$\dot{E}_{sm} = (\rho c)_m A \frac{\Delta x}{2} \frac{T_m' - T_m}{\Delta t} \quad (4\text{-}17)$$

Substituting Eqs. (4-16) and (4-17) into Eq. (4-15) and rearranging results in the equation

$$\frac{T_m' - T_m}{\Delta t} = \frac{k_{m-1} + k_m}{(\rho c)_m (\Delta x)^2}[T_{m-1} - T_m] - \frac{2q_L}{A(\rho c)_m \Delta x} . \tag{4-18}$$

Solving for the new temperature T_m' gives

$$T_m' = \frac{(k_{m-1} + k_m)\Delta t}{(\rho c)_m (\Delta x)^2} T_{m-1} + \left[1 - \frac{(k_{m-1} + k_m)\Delta t}{(\rho c)_m (\Delta x)^2}\right] T_m$$

$$- \frac{2q_L \Delta t}{(\rho c)_m A \Delta x} . \tag{4-19}$$

The finite-difference equations have now been derived. These equations are Eqs. (4-9), (4-14), and (4-19). To solve a heat transfer problem, the initial temperature of each of the m nodal points must be specified. This is identical to the specification of an initial condition for an analytically solved problem. To calculate the new temperature at time Δt, the heat-flux terms q_S and q_L must be specified. Equations (4-14) and (4-19) can then be used to determine the new boundary temperatures. The new temperature of each of the interior nodal points can be determined by solving Eq. (4-9) for each node. The resultant temperatures obtained for the m nodal points can then be used to calculate the temperatures at time $2\Delta t$. The iteration process is then continued to obtain the temperature at any desired future time.

Determination of Iteration Interval

The solution obtained by the finite-difference solution may differ from the correct solution. Errors introduced by using this method are classified as follows:[29]

(1) round-off errors

(2) errors due to the instability of the problem

(3) truncation errors.

Errors caused by "rounding-off" numbers can normally be disregarded since this type of error should statistically cancel itself out.

Instability may result if the time interval Δt is chosen too large. From physical reasoning, if the temperature of the nth node increases, the new temperature of the same node should also increase. Thus the derivative $\frac{dT_n'}{dT_n}$ must be positive. Taking the derivative of Eq. (4-9) with respect to T_n, one obtains

$$\frac{dT_n'}{dT_n} = 1 - \frac{(k_{n-1} + 2k_n + k_{n+1})\Delta t}{2(\rho c)_n(\Delta x)^2} . \qquad (4\text{-}20)$$

The requirement that Eq. (4-20) must be positive sets an upper limit on Δt. Thus

$$\Delta t \leq \frac{2(\rho c)_n(\Delta x)^2}{(K_{n-1} + 2K_n + K_{n+1})} . \qquad (4\text{-}21)$$

---

[29] Ibid., pp. 392-396.

Truncation errors result from the omission of the limit in the finite difference approximation. The truncation error can be considered by taking a Taylor series expansion of the function u(x) about the point x.[30] The truncation error is minimized if

$$\Delta t = \frac{(\Delta x)^2}{6\alpha} . \tag{4-22}$$

For a nonhomogeneous material

$$\Delta t = \frac{2(\rho c)_n (\Delta x)^2}{3(k_{n-1} + 2k_n + k_{n+1})} . \tag{4-23}$$

A computer program was written to evaluate Eqs. (4-9), (4-14), and (4-19). The operation of the finite-difference program can be checked by considering the original analytically solved problem. The analytically obtained results were given in Table 3-1. This problem assumed a constant surface heat flux and constant lower boundary temperatures for both soil profiles. The constant lower boundary temperature can be implemented in the finite-difference solution by using the relationship

$$T_m' = T_m \tag{4-24}$$

instead of Eq. (4-19).

Equation (4-21) requires that

$$\Delta t \leq 69 \text{ seconds} \tag{4-25}$$

for $\Delta x = 1$ cm and the thermal properties given in Chapter 3. Table 4-1 shows the results of the finite-difference solution of the heat transfer problem with $\Delta t = 60$ seconds.

---

[30] Ibid.

Table 4-1: Development of a Surface Thermal Anomaly With Time Using an Iteration Interval of 60 Seconds.

Elapsed Time (hrs.)	Surface Temperature of Profile A (°C)	Surface Temperature of Profile B (°C)	Percent of the Subsurface Thermal Anomaly Developed on the Surface
0	27.000	27.000	0
1	24.685	24.570	11.5
2	23.755	23.593	16.2
3	23.051	22.852	19.9
4	22.464	22.234	23.0
5	21.950	21.693	25.7
6	21.488	21.207	28.1
7	21.066	20.762	30.4
8	20.674	20.349	32.5
9	20.308	19.963	34.5

To minimize truncation errors, Eq. (4-23) requires that

$$\Delta t = 23 \text{ seconds.} \tag{4-26}$$

Table 4-2 shows the results of the finite-difference solution of the problem with Δt given by Eq. (4-26).

Comparison of Tables 4-1 and 4-2 shows that the larger time interval does not introduce any appreciable error. The results using the larger iteration interval are actually closer to the analytically obtained results. A 60 second iteration interval will therefore be used in all remaining problems.

Thermal Anomaly by Finite-Difference Model

Periodic variations in the surface heat flux must be considered in studying daily soil thermal properties. The daily surface heat flux may be approximated by the sum of the positive half of a sine wave during the day and a constant-loss term during day and night.[31] Since the primary temperature dependent heat-loss term is a radiative term, the surface heat flux approximation will be chosen to include a radiative term. The diurnal surface heat-flux term will thus be approximated by the sum of the positive half of a sine wave and a radiative-loss term. The radiation equation used will be the relationship by Fleagle given in Eq. (2-10).

---

[31] R. W. Smith Jr., RSL Report 69-4, Stanford, Calif., July 1969, pp. 21-22.

Table 4-2: Development of a Surface Thermal Anomaly With Time Using an Iteration Interval of 23 Seconds.

Elapsed Time (hrs.)	Surface Temperature of Profile A (°C)	Surface Temperature of Profile B (°C)	Percent of the Subsurface Thermal Anomaly Developed on the Surface
0	27.000	27.000	0
1	26.678	24.562	11.5
2	23.743	23.579	16.3
3	23.035	22.835	20.0
4	22.444	22.214	23.1
5	21.928	21.670	25.8
6	21.464	21.182	28.3
7	21.040	20.735	30.5
8	20.647	20.320	32.6
9	20.279	19.933	34.6

The form of the difference between the initial temperature profiles as a function of depth was previously found to be significant in its effect on the magnitude of the developing surface thermal anomaly. The finite-difference model will thus be used to evaluate the thermal profiles consistent with the model. The surface temperature of each profile and the surface thermal anomaly for a four day period are shown in Tables 4-3 through 4-6. A significant thermal anomaly develops within a few hours and is shown to be approximately 30 percent of the subsurface thermal anomaly present at a 50 cm depth for the thermal properties assumed. Daily variations in the surface anomaly are small compared with the magnitude of the surface thermal anomaly. Thus the initial assumption of identical initial surface temperatures is not reestablished even with a radiative temperature dependent surface heat flux.

The initial temperature profiles were assumed to exist at 1400 hours. Model corrections of this temperature profile are shown in Fig. 4-5. After 24 hours a new temperature profile is obtained which deviates from the initially assumed profile. This temperature profile at 1400 hours does not then deviate significantly for the last two days. Thus it represents a profile which is consistant with the model.

The temperature difference between profiles after four days is plotted in Fig. 4-6. An almost linear difference with depth can be seen. Thus the results in the previous model using a linear difference in initial temperature profiles appear valid for calculating the time of development of a surface thermal anomaly.

Table 4-3: Surface Thermal Anomaly During the First 24-Hour Period for a Clay Soil With 20-Volume-Percent Water.

Hours	Surface Temperature of Profile A (°C)	Surface Temperature of Profile B (°C)	Percent of the Subsurface Thermal Anomaly Developed on the Surface
1400	31.000	31.000	0.0
1500	30.631	30.536	9.4
1600	29.360	29.235	12.5
1700	27.377	27.232	14.6
1800	24.819	24.656	16.3
1900	23.196	23.019	17.7
2000	22.170	21.982	18.9
2100	21.395	21.196	19.9
2200	20.770	20.561	20.8
2300	20.246	20.030	21.7
0000	19.797	19.573	22.4
0100	19.404	19.173	23.1
0200	19.056	18.818	23.8
0300	18.743	18.499	24.4
0400	18.459	18.209	24.9
0500	18.200	17.945	25.5
0600	17.961	17.702	26.0
0700	19.105	18.841	26.4
0800	21.102	20.835	26.7
0900	23.387	23.117	27.0
1000	25.644	25.373	27.1
1100	27.629	27.356	27.3
1200	29.144	28.870	27.4
1300	30.046	29.770	27.6

Table 4-4: Surface Thermal Anomaly During the Second 24-Hour Period for a Clay Soil With 20-Volume-Percent Water.

Hours	Surface Temperature of Profile A (°C)	Surface Temperature of Profile B (°C)	Percent of the Subsurface Thermal Anomaly Developed on the Surface
1400	30.240	29.963	27.7
1500	29.688	29.408	27.9
1600	28.401	28.119	28.2
1700	26.442	26.158	28.5
1800	23.920	23.632	28.8
1900	22.336	22.045	29.1
2000	21.352	21.058	29.5
2100	20.618	20.320	29.7
2200	20.032	19.732	30.0
2300	19.546	19.244	30.3
0000	19.133	18.828	30.5
0100	18.774	18.467	30.7
0200	18.457	18.148	30.9
0300	18.175	17.864	31.1
0400	17.920	17.607	31.3
0500	17.689	17.374	31.5
0600	17.476	17.159	31.7
0700	18.645	18.328	31.8
0800	20.668	20.350	31.8
0900	22.977	22.660	31.8
1000	25.258	24.942	31.7
1100	27.265	26.950	31.5
1200	28.802	28.488	31.4
1300	29.724	29.410	31.3

Table 4-5: Surface Thermal Anomaly During the Third 24-Hour Period for a Clay Soil With 20-Volume-Percent Water.

Hours	Surface Temperature of Profile A (°C)	Surface Temperature of Profile B (°C)	Percent of the Subsurface Thermal Anomaly Developed on the Surface
1400	29.936	29.624	31.3
1500	29.400	29.088	31.3
1600	28.129	27.816	31.3
1700	26.184	25.870	31.5
1800	23.674	23.357	31.7
1900	22.103	21.784	31.9
2000	21.130	20.809	32.1
2100	20.406	20.084	32.2
2200	19.831	19.507	32.4
2300	19.355	19.030	32.5
0000	18.952	18.625	32.6
0100	18.602	18.274	32.7
0200	18.294	17.965	32.9
0300	18.020	17.690	33.0
0400	17.773	17.442	33.1
0500	17.548	17.217	33.1
0600	17.343	17.011	33.2
0700	18.519	18.187	33.3
0800	20.549	20.217	33.2
0900	22.865	22.534	33.1
1000	25.153	24.823	32.9
1100	27.166	26.838	32.7
1200	28.709	28.383	32.5
1300	29.635	29.312	32.4

Table 4-6: Surface Thermal Anomaly During the Fourth 24-Hour Period for a Clay Soil With 20-Volume-Percent Water.

Hours	Surface Temperature of Profile A (°C)	Surface Termperature of Profile B (°C)	Percent of the Subsurface Thermal Anomaly Developed on the Surface
1400	29.853	29.530	32.3
1500	29.322	29.000	32.2
1600	28.054	27.732	32.2
1700	26.113	25.790	32.3
1800	23.607	23.282	32.5
1900	22.039	21.712	32.6
2000	21.069	20.741	32.8
2100	20.348	20.019	32.9
2200	19.776	19.446	33.0
2300	19.303	18.972	33.1
0000	18.902	18.569	33.2
0100	18.554	18.221	33.3
0200	18.249	17.915	33.4
0300	17.977	17.642	33.5
0400	17.732	17.397	33.5
0500	17.510	17.174	33.6
0600	17.307	16.970	33.7
0700	18.485	18.148	33.7
0800	20.516	20.180	33.6
0900	22.834	22.499	33.4
1000	25.123	24.791	33.3
1100	27.138	26.808	33.1
1200	28.683	28.354	32.8
1300	29.611	29.284	32.7

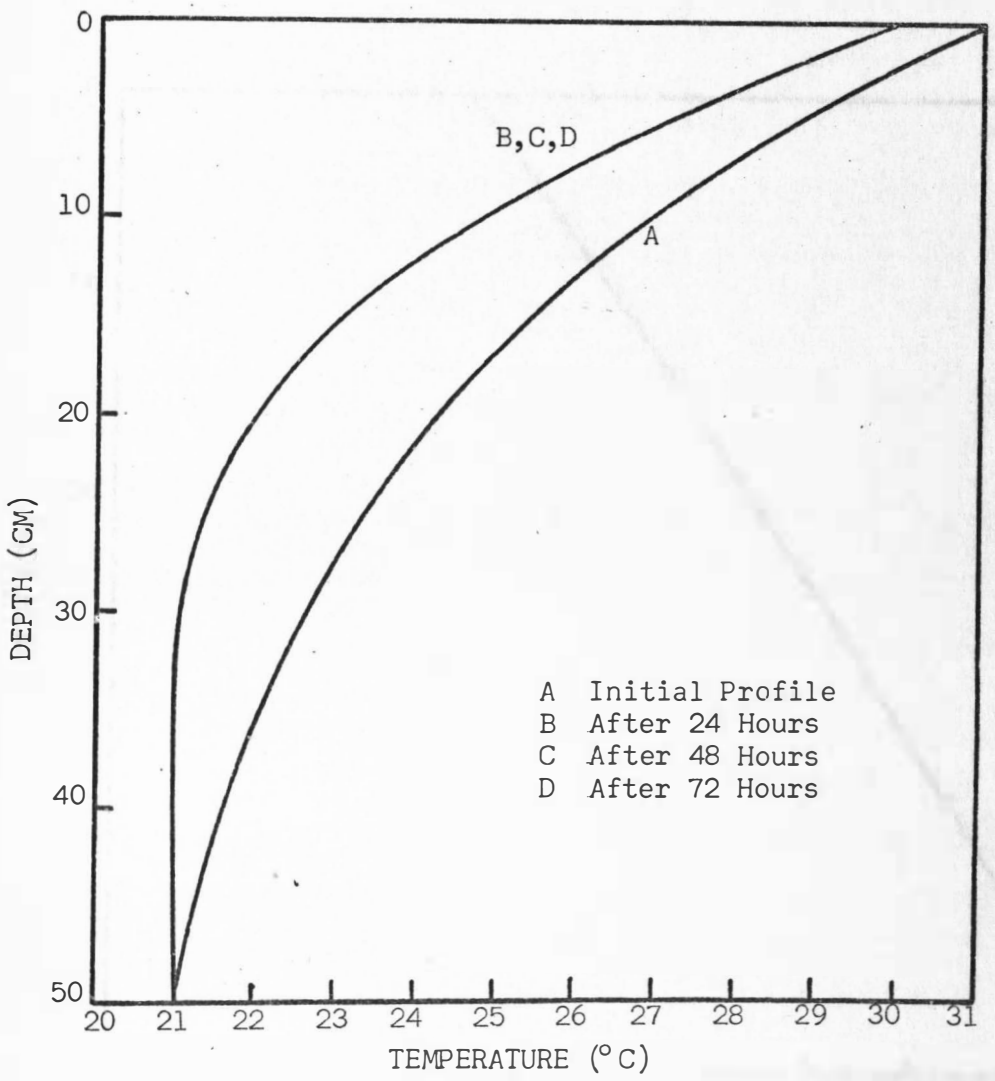

Fig. 4-5. Development of a Model Consistent Temperature Profile at 1400 Hours.

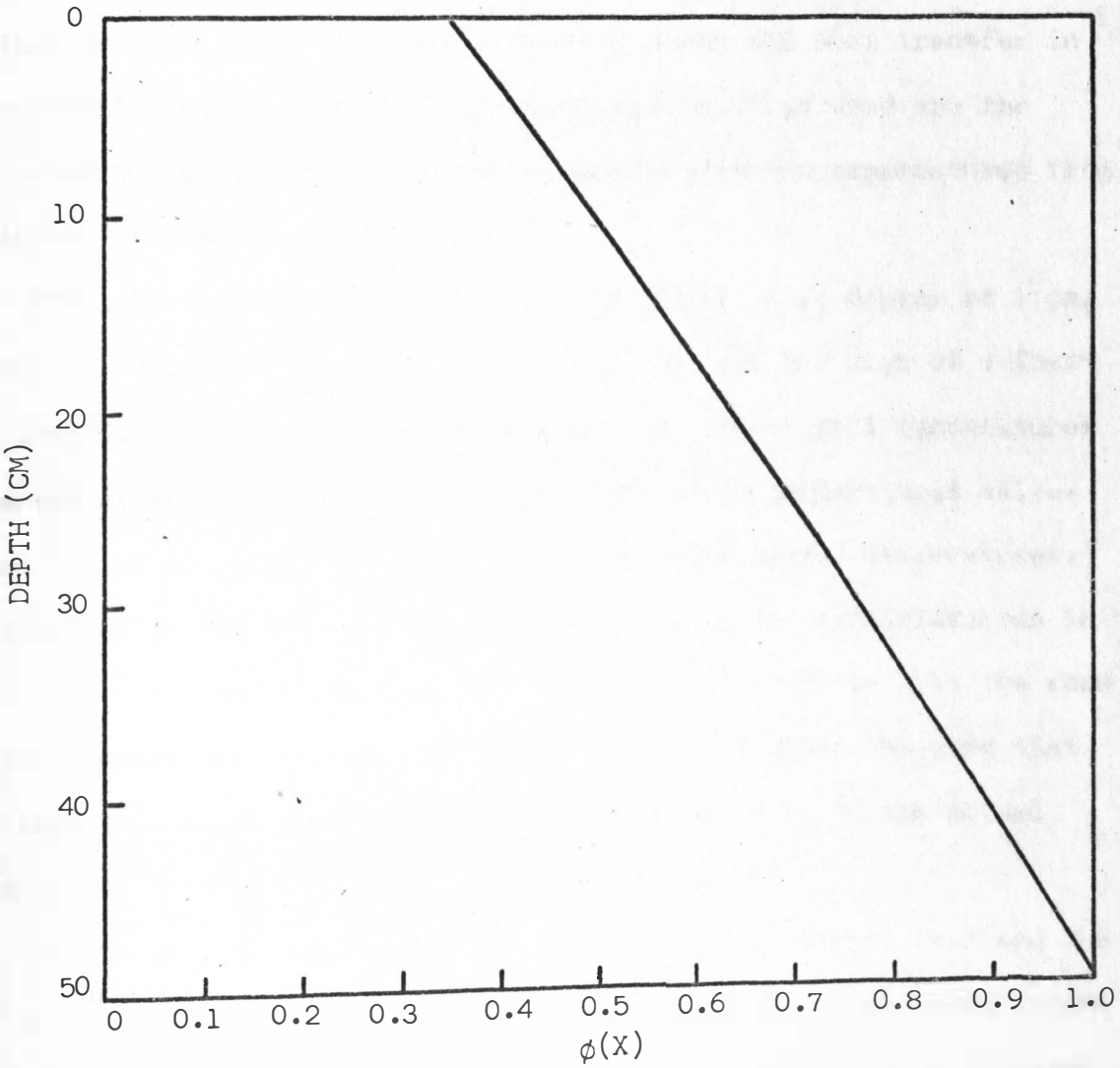

Fig. 4-6. Form of the Temperature Difference Between Temperature Profiles.

Validity of Lower Boundary Condition

The 50-cm temperature for both soil layers was previously assumed constant. To examine the validity of this assumption, the finite-difference computer program can be used to study the heat transfer in 100-cm soil layers. The initial temperature profiles used are the corrected 50-cm profiles obtained previously with the temperatures from 50 to 100 cm assumed initially equal.

The soil temperatures calculated for profile A at depths of 1 cm, 20 cm and 50 cm are shown in Fig. 4-7 for the last two days of a four-day period. Figure 4-8 shows 1-cm, 20-cm, and 50-cm soil temperatures measured at Argonne, Illinois. The periodic soil temperatures calculated by the computer compare in form with the measured temperatures. Differences in the numerical values are probably due to differences in heat flux and thermal properties. The important point is that the form of the temperature variation is similar in both figures implying that the heat flux terms used are probably a good estimate of the actual heat flux.

The 50-cm soil temperature fluctuations shown in Figs. 4-7 and 4-8 are small. The previous assumption of constant 50-cm soil temperatures therefore does not appear to greatly influence the previously obtained results.

The 50-cm thermal anomaly for four days is shown in Fig. 4-9. The anomaly can be seen to decrease rapidly at first with the rate of decrease becoming smaller with time. The change in the magnitude of the

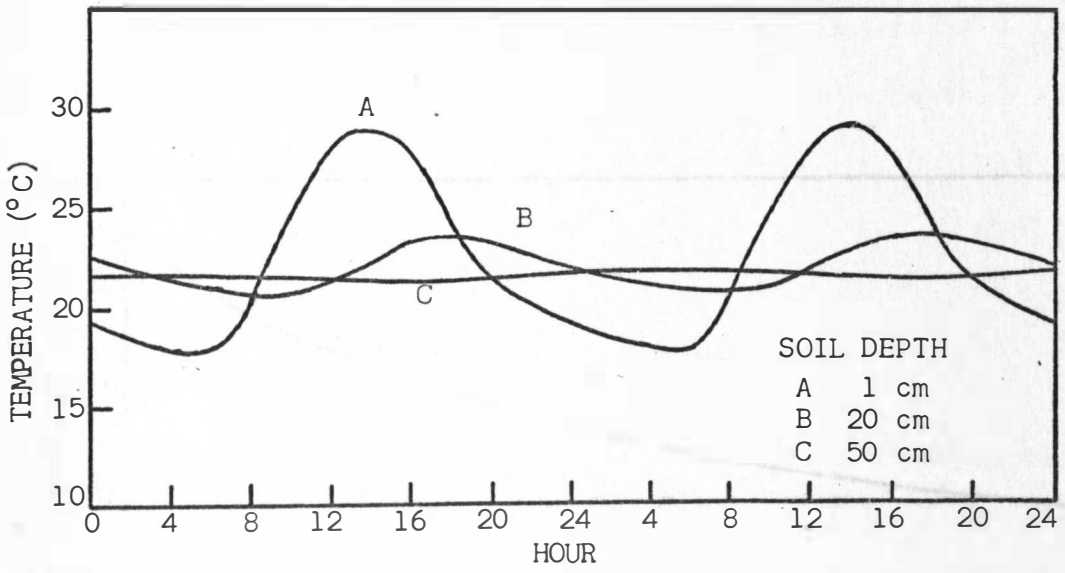

Fig. 4-7. Soil Temperatures Calculated With the Finite Difference Computer Program.

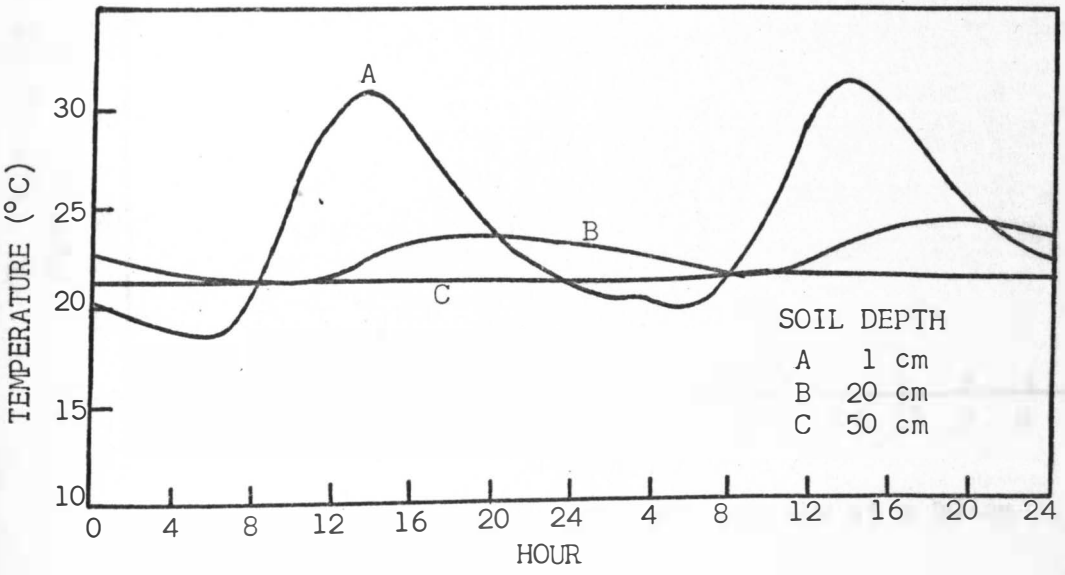

Fig. 4-8. Soil Temperatures Measured at Argonne, Illinois.*

*J. E. Carson, ANL Report 6470, Argonne, Illinois, Nov. 1961.

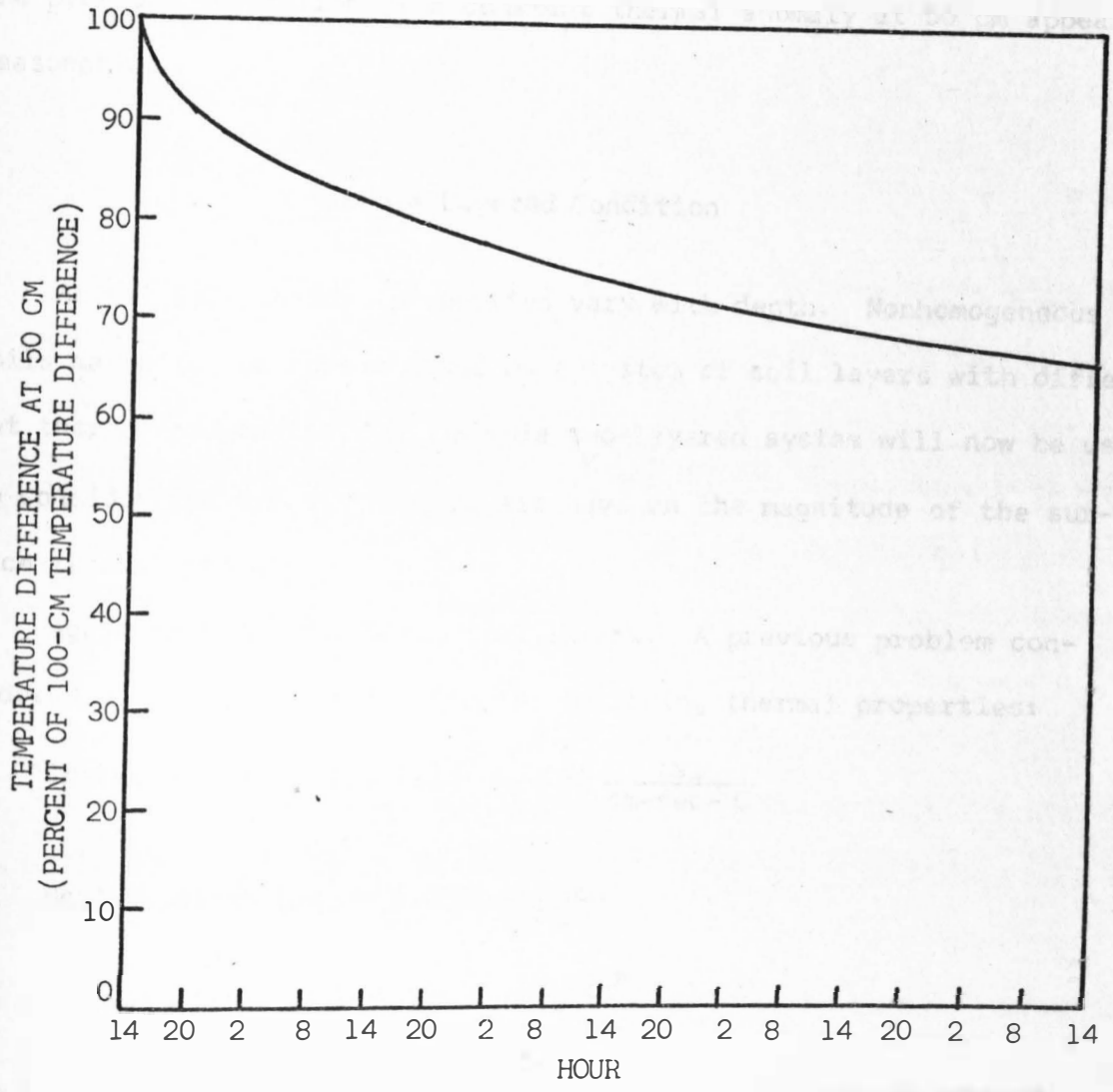

Fig. 4-9. Variation in the Thermal Anomaly at a 50-cm Depth.

50-cm anomaly was probably the result of the model correcting the initial profile. The important result is that no significant daily fluctuations occur in the subsurface anomaly at a 50-cm depth. Thus, the previous assumption of a constant thermal anomaly at 50 cm appears reasonable.

Simple Layered Condition

Actual soil thermal properties vary with depth. Nonhomogeneous soils may often be approximated by a system of soil layers with different thermal properties.[32] A simple two-layered system will now be used to consider the effect these layers have on the magnitude of the surface thermal anomaly.

Again consider two 50-cm soil layers. A previous problem considered a homogeneous soil with the following thermal properties:

Thermal conductivity (k) = $0.0036 \frac{\text{cal}}{\text{cm-sec-}^{\circ}\text{C}}$

Heat capacity (ρc) = $0.5000 \frac{\text{cal}}{\text{cm}^3\text{-}^{\circ}\text{C}}$

Thermal diffusivity (α) = $0.0072 \frac{\text{cm}^2}{\text{sec}}$.

The above values were given for a clay soil with 20-volume-percent water. The surface soil temperature variations and surface thermal anomaly for four days is shown in Tables 4-3 through 4-6.

---

[32] W. R. vanWijk and W. J. Derksen, in Physics of Plant Evviron-ment, W. R. vanWijk, Ed., (North-Holland Publishing Co., Amsterdam, 1963), pp. 171-209.

A clay soil with 40-volume-percent water has the following thermal properties:[33]

Thermal conductivity (k) = 0.0043 $\frac{\text{cal}}{\text{cm-sec-}^{\circ}\text{C}}$

Heat capacity (ρc) = 0.7049 $\frac{\text{cal}}{\text{cm}^3\text{-}^{\circ}\text{C}}$

Thermal diffusivity (α) = 0.0061 $\frac{\text{cm}^2}{\text{sec}}$.

The results obtained by considering homogeneous soil profiles with the above stated thermal properties for a clay soil with 40-volume-percent water are included in Tables 4-7 through 4-10.

Comparison of the tables for the two different homogeneous soils shows that a slightly larger surface thermal anomaly develops in the soil containing more water. The daily variation in the thermal anomaly does not appear to be affected by the difference in soil thermal properties.

Now consider a simple two-layered system. Assume that the near-surface soil thermal properties can be approximated by a 25-cm homogeneous soil layer with 20-volume-percent water above a 25-cm homogeneous soil layer with 40-volume-percent water. The results obtained from this layered system are contained in Tables 4-11 through 4-14. The results obtained by interchanging the layers is contained in Tables 4-15 through 4-18.

---

[33] Geiger, loc. cit., p. 171.

Table 4-7: Surface Thermal Anomaly During the First 24-Hour Period for a Clay Soil With 40-Volume-Percent Water.

Hours	Surface Temperature of Profile A (°C)	Surface Temperature of Profile B (°C)	Percent of the Subsurface Thermal Anomaly Developed on the Surface
1400	31.000	31.000	0.0
1500	30.357	30.267	9.0
1600	29.242	29.121	12.1
1700	27.578	27.435	14.3
1800	25.449	25.289	16.0
1900	24.046	23.871	17.5
2000	23.128	22.940	18.7
2100	22.419	22.221	19.9
2200	21.839	21.630	20.8
2300	21.347	21.130	21.8
0000	20.921	20.695	22.6
0100	20.544	20.311	23.3
0200	20.208	19.967	24.1
0300	19.904	19.657	24.7
0400	19.627	19.373	25.3
0500	19.372	19.113	25.9
0600	19.137	18.872	26.5
0700	19.995	19.725	27.0
0800	21.560	21.286	27.4
0900	23.384	23.107	27.8
1000	25.215	24.934	28.1
1100	26.849	26.565	28.4
1200	28.123	27.837	28.6
1300	28.911	28.622	28.9

Table 4-8: Surface Thermal Anomaly During the Second 24-Hour Period for a Clay Soil With 40-Volume-Percent Water.

Hours	Surface Temperature of Profile A (°C)	Surface Temperature of Profile B (°C)	Percent of the Subsurface Thermal Anomaly Developed on the Surface
1400	29.129	28.837	29.1
1500	28.736	28.442	29.4
1600	27.737	27.440	29.7
1700	26.177	25.877	30.0
1800	24.140	23.837	30.4
1900	22.819	22.511	30.7
2000	21.975	21.664	31.1
2100	21.332	21.018	31.4
2200	20.812	20.495	31.7
2300	20.375	20.055	32.0
0000	19.999	19.676	32.3
0100	19.668	19.343	32.6
0200	19.374	19.046	32.8
0300	19.110	18.779	33.0
0400	18.869	18.536	33.3
0500	18.649	18.314	33.5
0600	18.446	18.109	33.7
0700	19.335	18.997	33.9
0800	20.931	20.591	34.0
0900	22.784	22.444	34.0
1000	24.643	24.303	34.1
1100	26.305	25.964	34.1
1200	27.604	27.264	34.0
1300	28.417	28.076	34.0

Table 4-9: Surface Thermal Anomaly During the Third 24-Hour Period for a Clay Soil With 40-Volume-Percent Water.

Hours	Surface Temperature of Profile A (°C)	Surface Temperature of Profile B (°C)	Percent of the Subsurface Thermal Anomaly Developed on the Surface
1400	28.657	28.317	34.1
1500	28.286	27.945	34.1
1600	27.306	26.964	34.2
1700	25.764	25.421	34.4
1800	23.744	23.399	34.5
1900	22.438	22.091	34.7
2000	21.609	21.260	34.9
2100	20.982	20.631	35.1
2200	20.476	20.123	35.3
2300	20.052	19.698	35.4
0000	19.689	19.333	35.6
0100	19.371	19.014	35.7
0200	19.089	18.731	35.8
0300	18.836	18.476	35.9
0400	18.606	18.246	36.1
0500	18.397	18.035	36.2
0600	18.204	17.841	36.3
0700	19.104	18.740	36.3
0800	20.709	20.345	36.3
0900	22.573	22.210	36.3
1000	24.441	24.079	36.2
1100	26.112	25.751	36.1
1200	27.420	27.060	36.0
1300	28.241	27.882	35.9

Table 4-10: Surface Thermal Anomaly During the Fourth 24-Hour Period for a Clay Soil With 40-Volume-Percent Water.

Hours	Surface Temperature of Profile A (°C)	Surface Temperature of Profile B (°C)	Percent of the Subsurface Thermal Anomaly Developed on the Surface
1400	28.490	28.131	35.8
1500	28.125	27.767	35.8
1600	27.153	26.794	35.8
1700	25.617	25.258	35.9
1800	23.603	23.242	36.0
1900	22.302	21.940	36.2
2000	21.479	21.116	36.3
2100	20.856	20.492	36.4
2200	20.355	19.990	36.5
2300	19.937	19.570	36.6
0000	19.578	19.211	36.7
0100	19.265	18.896	36.8
0200	18.987	18.618	36.9
0300	18.738	18.368	37.0
0400	18.512	18.142	37.1
0500	18.307	17.935	37.1
0600	18.117	17.745	37.2
0700	19.021	18.648	37.2
0800	20.630	18.258	37.2
0900	22.497	22.126	37.1
1000	24.369	23.999	37.0
1100	26.043	25.674	36.8
1200	27.355	26.987	36.7
1300	28.178	27.812	36.6

Table 4-11: Surface Thermal Anomaly During the First 24-Hour Period With a Layer of Clay Soil With 20-Volume-Percent Water Over a Layer of Clay Soil With 40-Volume-Percent Water.

Hours	Surface Temperature of Profile A (°C)	Surface Temperature of Profile B (°C)	Percent of the Subsurface Thermal Anomaly Developed on the Surface
1400	31.000	31.000	0.0
1500	30.631	30.536	9.4
1600	29.358	29.234	12.5
1700	27.372	27.226	14.6
1800	24.807	24.643	16.4
1900	23.174	22.995	17.9
2000	22.138	21.946	19.2
2100	21.351	21.148	20.3
2200	20.715	20.501	21.3
2300	20.182	19.959	22.3
0000	19.725	19.494	23.1
0100	19.327	19.089	23.9
0200	18.976	18.730	24.6
0300	18.662	18.410	25.3
0400	18.380	18.121	25.9
0500	18.124	17.859	26.5
0600	17.890	17.620	27.0
0700	19.040	18.765	27.5
0800	21.044	20.766	27.9
0900	23.337	23.056	28.1
1000	25.603	25.319	28.4
1100	27.596	27.310	28.5
1200	29.120	28.833	28.7
1300	30.028	29.740	28.9

Table 4-12: Surface Thermal Anomaly During the Second 24-Hour Period With a Layer of Clay Soil With 20-Volume-Percent Water Over a Layer of Clay Soil With 40-Volume-Percent Water.

Hours	Surface Temperature of Profile A (°C)	Surface Temperature of Profile B (°C)	Percent of the Subsurface Thermal Anomaly Developed on the Surface
1400	30.228	29.937	29.0
1500	29.678	29.385	29.3
1600	28.391	28.096	29.5
1700	26.430	26.131	29.8
1800	23.902	23.600	30.2
1900	22.311	22.005	30.6
2000	21.318	21.008	30.9
2100	20.573	20.261	31.3
2200	19.978	19.663	31.6
2300	19.484	19.166	31.8
0000	19.064	18.743	32.1
0100	18.701	18.378	32.3
0200	18.382	18.056	32.6
0300	18.099	17.772	32.8
0400	17.846	17.516	33.0
0500	17.618	17.286	33.2
0600	17.410	17.076	33.4
0700	18.585	18.250	33.5
0800	20.615	20.280	33.5
0900	22.932	22.597	33.5
1000	25.221	24.888	33.4
1100	27.237	26.904	33.2
1200	28.782	28.451	33.1
1300	29.710	29.380	33.0

Table 4-13: Surface Thermal Anomaly During the Third 24-Hour Period With a Layer of Clay Soil With 20-Volume-Percent Water Over a Layer of Clay Soil With 40-Volume-Percent Water.

Hours	Surface Temperature of Profile A (°C)	Surface Temperature of Profile B (°C)	Percent of the Subsurface Thermal Anomaly Developed on the Surface
1400	29.928	29.598	33.0
1500	29.394	29.065	33.0
1600	28.123	27.792	33.0
1700	26.175	25.843	33.2
1800	23.659	23.325	33.4
1900	22.080	21.744	33.6
2000	21.098	20.760	33.8
2100	20.365	20.025	34.0
2200	19.780	19.438	34.1
2300	19.296	18.953	34.3
0000	18.885	18.541	34.4
0100	18.531	18.185	34.6
0200	18.220	17.874	34.7
0300	17.946	17.598	34.8
0400	17.700	17.351	34.9
0500	17.479	17.129	35.0
0600	17.278	16.928	35.1
0700	18.461	18.109	35.1
0800	20.297	20.146	35.1
0900	22.821	22.471	34.9
1000	25.117	24.769	34.7
1100	27.138	26.793	34.5
1200	28.689	28.346	34.3
1300	29.623	29.281	34.2

Table 4-14: Surface Thermal Anomaly During the Fourth 24-Hour Period With a Layer of Clay Soil With 20-Volume-Percent Water Over a Layer of Clay Soil With 40-Volume-Percent Water.

Hours	Surface Temperature of Profile A (°C)	Surface Temperature of Profile B (°C)	Percent of the Subsurface Thermal Anomaly Developed on the Surface
1400	29.845	29.504	34.1
1500	29.316	28.976	34.0
1600	28.049	27.709	34.0
1700	26.105	25.764	34.1
1800	23.593	23.250	34.3
1900	22.017	21.672	34.5
2000	21.038	20.692	34.6
2100	20.307	19.960	34.7
2200	19.725	19.376	34.9
2300	19.244	18.894	35.0
0000	18.836	18.485	35.1
0100	18.484	18.132	35.2
0200	18.176	17.823	35.3
0300	17.903	17.550	35.3
0400	17.660	17.306	35.4
0500	17.441	17.086	35.5
0600	17.242	16.887	35.6
0700	18.426	18.071	35.6
0800	20.464	20.110	35.5
0900	20.790	20.437	35.3
1000	25.088	24.737	35.1
1100	27.111	26.762	34.9
1200	28.663	28.317	34.7
1300	29.598	29.253	34.5

Table 4-15: Surface Thermal Anomaly During the First 24-Hour Period With a Layer of Clay Soil With 40-Volume-Percent Water Over a Layer of Clay Soil With 20-Volume-Percent Water.

Hours	Surface Temperature of Profile A (°C)	Surface Temperature of Profile B (°C)	Percent of the Subsurface Thermal Anomaly Developed on the Surface
1400	31.000	31.000	0.0
1500	30.357	30.267	9.0
1600	29.242	29.121	12.1
1700	27.581	27.438	14.2
1800	25.457	25.298	15.9
1900	24.061	23.888	17.3
2000	23.152	22.967	18.5
2100	22.453	22.258	19.5
2200	21.883	21.679	20.4
2300	21.401	21.188	21.2
0000	20.983	20.763	22.0
0100	20.614	20.388	22.7
0200	20.284	20.051	23.3
0300	19.984	19.745	23.9
0400	19.710	19.465	24.4
0500	19.456	19.207	24.9
0600	19.221	18.967	25.4
0700	20.078	19.819	25.9
0800	21.640	21.378	26.2
0900	23.461	23.195	26.6
1000	25.287	25.018	26.8
1100	26.916	26.645	27.1
1200	28.184	27.911	27.3
1300	28.967	28.692	27.5

Table 4-16: Surface Thermal Anomaly During the Second 24-Hour Period With a Layer of Clay Soil With 40-Volume-Percent Water Over a Layer of Clay Soil With 20-Volume-Percent Water.

Hours	Surface Temperature of Profile A (°C)	Surface Temperature of Profile B (°C)	Percent of the Subsurface Thermal Anomaly Developed on the Surface
1400	29.180	28.903	27.7
1500	28.784	28.504	28.0
1600	27.782	27.500	28.2
1700	26.222	25.936	28.5
1800	24.186	23.898	28.8
1900	22.867	22.576	29.2
2000	22.027	21.732	29.5
2100	21.390	21.092	29.8
2200	20.876	20.575	30.1
2300	20.444	20.141	30.3
0000	20.073	19.767	30.6
0100	19.747	19.439	30.8
0200	19.456	19.146	31.0
0300	19.194	18.881	31.3
0400	18.954	18.639	31.5
0500	18.733	18.416	31.7
0600	18.528	18.209	31.9
0700	19.415	19.095	32.0
0800	21.007	20.685	32.1
0900	22.856	22.534	32.2
1000	24.709	24.307	32.2
1100	26.365	26.043	32.2
1200	27.659	27.337	32.2
1300	28.465	28.144	32.2

Table 4-17: Surface Thermal Anomaly During the Third 24-Hour Period With a Layer of Clay Soil With 40-Volume-Percent Water Over a Layer of Clay Soil With 20-Volume-Percent Water.

Hours	Surface Temperature of Profile A (°C)	Surface Temperature of Profile B (°C)	Percent of the Subsurface Thermal Anomaly Developed on the Surface
1400	28.701	28.379	32.2
1500	28.326	28.003	32.2
1600	27.343	27.020	32.3
1700	25.800	25.476	32.4
1800	23.781	23.455	32.6
1900	22.478	22.150	32.8
2000	21.653	21.323	33.0
2100	21.031	20.699	33.1
2200	20.530	20.198	33.3
2300	20.113	19.778	33.4
0000	19.754	19.419	33.6
0100	19.441	19.104	33.7
0200	19.162	18.824	33.8
0300	18.911	18.572	33.9
0400	18.683	18.342	34.0
0500	18.473	18.131	34.1
0600	18.278	17.936	34.2
0700	19.175	18.832	34.3
0800	20.777	20.434	34.3
0900	22.636	22.294	34.2
1000	24.499	24.158	34.2
1100	26.165	25.824	34.1
1200	27.468	27.128	34.0
1300	28.283	27.944	33.9

Table 4-18: Surface Thermal Anomaly During the Fourth 24-Hour Period With a Layer of Clay Soil With 40-Volume-Percent Water Over a Layer of Clay Soil With 20-Volume-Percent Water.

Hours	Surface Temperature of Profile A (°C)	Surface Temperature of Profile B (°C)	Percent of the Subsurface Thermal Anomaly Developed on the Surface
1400	28.526	28.188	33.8
1500	28.158	27.820	33.8
1600	27.183	26.845	33.8
1700	25.647	25.308	33.9
1800	23.634	23.293	34.0
1900	22.336	21.994	34.2
2000	21.517	21.174	34.3
2100	20.900	20.556	34.4
2200	40.404	20.060	34.5
2300	19.991	19.646	34.6
0000	19.638	19.291	34.7
0100	19.329	18.982	34.7
0200	19.055	18.707	34.8
0300	18.808	18.459	34.9
0400	18.584	18.234	35.0
0500	18.377	18.027	35.0
0600	18.187	17.836	35.1
0700	19.088	18.736	35.1
0800	20.693	20.342	35.1
0900	22.556	22.206	35.0
1000	24.423	24.074	34.9
1100	26.091	25.744	34.8
1200	27.398	27.051	34.6
1300	28.216	27.871	34.5

Tables 4-14 and 4-18 show the results during the fourth day for both layer conditions. The surface thermal anomaly for each layered condition is almost identical. Furthermore, the magnitude of the surface thermal anomaly is midway between the magnitudes obtained for the homogeneous problems as shown in Tables 4-6 and 4-10. Thus a layered system with thermal properties only moderately different from each other may give results similar to those which might be obtained using a homogeneous material with average thermal properties.

Analysis of Radiation Term

The finite-difference model assumes a diurnal heat flux approximated by the sum of the positive half of a sine wave and a radiative-loss term. The radiative-loss term as proposed by Fleagle requires the specification of a temperature T' representing the effect of the atmospheric absorption and reradiation of energy. The temperature T' was previously held constant at 10° C which resulted in an energy loss similar in magnitude with experimental measurements.[34]

Consider now the effect the value of T' has on the magnitude of the surface thermal anomaly. Consider the development of the surface thermal anomaly from the corrected profiles obtained previously. Tables 4-19 through 4-22 show the results for different values of T'.

---

[34] H. H. Lettau and B. Davidson, Ed., Exploring the Atmosphere's First Mile, Vol. 2, (Pergamon Press, London, 1957).

Table 4-19: Surface Temperatures and Surface Thermal Anomaly With $T' = 30^{\circ}C$.

Hours	Surface Temperature of Profile A (°C)	Surface Temperature of Profile B (°C)	Percent of the Subsurface Thermal Anomaly Developed on the Surface
1400	29.830	29.505	32.5
1500	32.962	32.639	32.3
1600	32.873	32.552	32.1
1700	31.746	31.425	32.1
1800	29.883	29.562	32.1
1900	28.850	28.528	32.2
2000	28.335	28.013	32.2
2100	28.009	27.687	32.2
2200	27.787	27.464	32.2
2300	27.628	27.305	32.3
0000	27.511	27.188	32.3
0100	27.423	27.100	32.3
0200	27.356	27.034	32.3
0300	27.305	26.983	32.3
0400	27,266	26.943	32.3
0500	27.235	26.912	32.3
0600	27.211	26.888	32.3

Table 4-20: Surface Temperatures and Surface Thermal Anomaly With T' = 10°C.

Hours	Surface Temperature of Profile A (°C)	Surface Temperature of Profile B (°C)	Percent of the Subsurface Thermal Anomaly Developed on the Surface
1400	29.830	29.505	32.5
1500	29.300	28.975	32.5
1600	28.034	27.709	32.5
1700	26.094	25.769	32.5
1800	23.588	23.261	32.7
1900	22.021	21.692	32.9
2000	21.052	20.722	33.0
2100	20.332	20.001	33.1
2200	19.761	19.429	33.2
2300	19.289	18.956	33.3
0000	18.888	18.554	33.4
0100	18.541	18.207	33.5
0200	18.237	17.901	33.5
0300	17.965	17.629	33.6
0400	17.721	17.384	33.7
0500	17.499	17.162	33.7
0600	17.297	16.959	33.8

Table 4-21: Surface Temperatures and Surface Thermal Anomaly With T' = - 10°C.

Hours	Surface Temperature of Profile A (°C)	Surface Temperature of Profile B (°C)	Percent of the Subsurface Thermal Anomaly Developed on the Surface
1400	29.830	29.505	32.5
1500	26.323	25.997	32.6
1600	24.084	23.757	32.8
1700	21.467	21.137	32.9
1800	18.420	18.088	33.2
1900	16.399	16.065	33.4
2000	15.043	14.706	33.6
2100	13.982	13.644	33.8
2200	13.108	12.767	34.0
2300	12.362	12.020	34.2
0000	11.712	11.368	34.3
0100	11.136	10.791	34.5
0200	10.619	10.273	34.6
0300	10.150	9.803	34.7
0400	9.722	9.373	34.9
0500	9.327	8.987	35.0
0600	8.962	8.611	35.1

Table 4-22: Surface Temperatures and Surface Thermal Anomaly With T' = - 30°C.

Hours	Surface Temperature of Profile A (°C)	Surface Temperature of Profile B (°C)	Percent of the Subsurface Thermal Anomaly Developed on the Surface
1400	29.830	29.505	32.5
1500	23.944	23.616	32.8
1600	20.918	20.589	33.0
1700	17.748	17.415	33.2
1800	14.257	13.921	33.6
1900	11.861	11.522	33.9
2000	10.182	9.840	34.2
2100	8.837	8.493	34.4
2200	7.707	7.360	34.7
2300	6.730	6.381	34.9
0000	5.867	5.517	35.1
0100	5.095	4.743	35.3
0200	4.397	4.042	35.5
0300	3.758	3.401	35.6
0400	3.170	2.812	35.8
0500	2.625	2.265	36.0
0600	2.118	1.757	36.1

Although the surface temperatures differ considerably for different values of T', the surface thermal anomaly changes little. Thus the surface thermal anomaly appears insensitive to the value of T'.

CHAPTER 5. SUMMARY OF RESULTS

Two models were developed to simulate heat transfer in the upper soil region. The development of a surface thermal anomaly from a subsurface anomaly was studied by considering two soil layers with slightly different thermal profiles. The thermal properties of the soil and the surface heat flux were varied to determine their effect on the magnitude of the surface thermal anomaly.

The first model simulated nocturnal soil temperatures assuming a constant heat loss equal for both soil layers. Analytical solution of the heat transfer problem showed that the surface thermal anomaly was independent of the surface heat flux.

Evaluation of the solution obtained showed the development of a significant surface thermal anomaly after a few hours. The magnitude of the surface thermal anomaly developed was found to be dependent only on the form of the difference between initial temperature profiles, the soil thermal diffusivity, and the magnitude of the subsurface thermal anomaly. The magnitude of the surface thermal anomaly was also found to approach the magnitude of the subsurface thermal anomaly as the elapsed time increased. This result contradicts the initial assumption that the surface thermal anomaly would disappear during the day and reappear during the night.

The second model simulated diurnal soil temperatures. A radiative-heat-loss term was included in the periodic heat-flux term to determine if this would reduce the magnitude of the surface thermal anomaly. A finite-difference computer program was then written to calculate the soil temperatures throughout the day.

A significant surface thermal anomaly was found to again develop within a few hours. This anomaly continued to increase in magnitude approaching a nearly constant value after three days. Daily fluctuations of the anomaly were small compared to its magnitude.

The new temperature profiles at 1400 hours were found to deviate from the initial 1400-hour temperature profiles selected. After several days, the 1400-hour profiles appeared to become consistent with the model.

The surface thermal anomaly calculated in the first model was found to be highly dependent on the form of the difference between initial temperature profiles. The results of the second model, though, showed a corrected difference between thermal profiles which was approximately linear with depth. Therefore, the assumption of a linear difference between profiles appears valid.

The soil temperatures at a 50-cm depth were held constant in both models. The validity of this assumption was considered by extending the second model to a depth of 100 cm. The fluctuation in the 50-cm soil temperatures was found to be small compared to the daily surface temperature fluctuations. Thus the assumption of constant 50-cm temperatures did not appear to significantly affect the results.

A simple layered soil was also considered. The 50-cm thick soil layers were divided into two homogeneous layers of equal thickness. Different soil thermal properties were then assigned to each layer. The results obtained for the layered soil appear to be similar to the results which would be expected using homogeneous 50-cm thick layers with average thermal properties.

CHAPTER 6. CONCLUSIONS

The two simulation models suggest that a significant surface thermal anomaly will develop in a few hours. A radiative temperature dependent heat-flux term will decrease the magnitude of the surface thermal anomaly but will not destroy it. A highly temperature dependent heat-flux term appears to be needed to eliminate the surface thermal anomaly.

The surface thermal anomaly also appears to be insensitive to variations in the surface heat flux. Its magnitude was found to fluctuate only a few percent throughout a diurnal cycle.

APPENDIX

Finite-Difference Computer Program

A FORTRAN computer program was written for the IBM 360/40 computer. The program was used to evaluate the soil temperatures in the second simulation model. The program reads in values for the thermal conductivity, specific heat, and initial temperature distributions for both soil layers. The surface heat flux is then calculated by the subroutine QHEAT. Evaluation of the Eqs. (4-9), (4-14) and (4-19) then determines the new temperature of each nodal point. The program then prints out the results after a predetermined number of calculations have been performed.

Description of Major Programming Symbols

Symbol used in program	Symbol used in text
DX	Δx
DT	Δt
K(I)	k_n
SH(I)	$(\rho c)_n$
TA(I)	$(T_A)_n$
TB(I)	$(T_B)_n$
SA(I)	$(T_A)'_n$
SB(I)	$(T_B)'_n$
ST	$(T_A)_1-(T_B)_1$
QC	$(q_A)_s$
QD	$(q_B)_s$

```
C
C     ****************************************************************
C     *  DX IS THE DISTANCE INTERVAL BETWEEN NODAL POINTS IN         *
C     *       CENTIMETERS                                           *
C     *  DT IS THE TIME INTERVAL BETWEEN CALCULATIONS IN SECONDS     *
C     *  M IS THE NUMBER OF EQUALLY SPACED NODAL POINTS              *
C     *  IJ IS THE NUMBER OF PROBLEMS TO BE SOLVED                   *
C     *  IK=1 IF CONDUCTIVITY AND DIFFUSIVITY VALUES ARE TO BE READ IN*
C     *     2 IF CONDUCTIVITY AND DIFFUSIVITY VALUES ARE TO BE       *
C     *       CALCULATED                                            *
C     *  PIT IS THE TIME INTERVAL BETWEEN PRINTOUTS IN MINUTES       *
C     *  CHR IS THE INITIAL STARTING HOUR                            *
C     *  CMIN IS THE INITIAL STARTING MINUTE                         *
C     *  EDAY IS THE NUMBER OF DAYS AFTER THE INITIAL DAY WHEN THE   *
C     *       CALCULATION IS TO STOP                                 *
C     *  EHR IS THE HOUR WHEN THE CALCULATION IS TO END              *
C     *  EMIN IS THE MINUTE WHEN THE CALCULATION IS TO END           *
C     ****************************************************************
C
C
      DOUBLE PRECISION AAI,AI(120),K(120),SH(120),AA(120),BA(120),
     2CA(120),AB,CB,AC,CC,SA(120),SB(120),TA(120),TB(120),ST,B,TTA,TTB,
     3X,BBB,BB,RA(120),RB(120)
      KKK=1
   60 READ(11,101) DX,DT,M,IJ,IK,PIT,CHR,CMIN,EDAY,EHR,EMIN
  101 FORMAT(2(F4.0),3I3,6(F3.0))
      READ(11,404) TAI
  404 FORMAT(F6.2)
      L=0.0
      J=0.0
      NN=0.0
      NAC=0
      N=M-1
      DAY=0.0
      TIME=0.0
      J=0
C     SPECIFICATION OF INITIAL TEMPERATURE PROFILE
      DO 403 I=1,M
  403 READ(13,402) TA(I),TB(I)
      QC=0.000
      QD=0.000
      ST=TA(1)-TB(1)
   30 J=J&1
      IF(IK.NE.1) GO TO 4
      IF(J.GT.1) GO TO 17
```

```
C     READ VALUES FOR CONDUCTIVITY AND SPECIFIC HEAT
      READ(11,102) Y,Z
  102 FORMAT(2(F6.4))
      DO 7 I=1,M
      K(I)=Y
    7 SH(I)=Z
      GO TO 9
    4 CONTINUE
C     IF CONDUCTIVITY AND SPECIFIC HEAT ARE TIME DEPENDENT,
C     CALCULATION SUBROUTINE GOES HERE
    9 CONTINUE
    5 AAI=DT/(2*DX*DX)
    3 DO 8 I=1,M
    8 AI(I)=AAI/SH(I)
      GO TO 25
   17 CONTINUE
C     CALL SUBROUTINE TO CALCULATE THE SURFACE HEAT FLUX
      CALL QHEAT (QA,QB,QC,QD,DT,DX,TA,TB,J,K,M,CHR,CMIN,TAI)
C     CALCULATION OF INTERNAL NODAL TEMPERATURES
      DO 10 I=2,N
      SA(I)=AI(I)*((K(I-1)&K(I))*TA(I-1)&(1/AI(I)-K(I-1)-2*K(I)-K(I&1))
     7*TA(I)&(K(I)&K(I&1))*TA(I&1))
   10 SB(I)=AI(I)*((K(I-1)&K(I))*TB(I-1)&(1/AI(I)-K(I-1)-2*K(I)-K(I&1))
     6*TB(I)&(K(I)&K(I&1))*TB(I&1))
C     CALCULATION OF SURFACE NODAL TEMPERATURES
      SA(1)=AI(1)*(4*DX*QC&(1/AI(1)-2*K(1)-2*K(2))*TA(1)&(2*K(1)&2*K(2))
     8*TA(2))
      SB(1)=AI(1)*(4*DX*QD&(1/AI(1)-2*K(1)-2*K(2))*TB(1)&(2*K(1)&2*K(2))
     9*TB(2))
C     CALCULATION OF LOWER BOUNDARY TEMPERATURES
      SA(M)=TA(M)
      SB(M)=TB(M)
C     REASSIGNMENT OF NODAL TEMPERATURES FOR NEXT ITERATION
      DO 15 I=1,M
      TA(I)=SA(I)
   15 TB(I)=SB(I)
      IF(TIME.LT.PIT) GO TO 40
      ST=TA(1)-TB(1)
C     THIS PORTION OF THE PROGRAM WRITES OUT THE PERTINENT DATA
   25 NHR=CHR
      NMIN=CMIN
      IF(M.GT.52) GO TO 56
      NN=NN&1
      NAN=NN/2
      NAB=NAN*2
      IF(NAB.EQ.NN) GO TO 58
```

```
 56 WRITE(12,200)
200 FORMAT(1H1)
 58 IF(NHR.GE.9) GO TO 51
    IF(NMIN.GE.9) GO TO 57
    WRITE(12,104) NAC,NHR,NAC,NMIN
104 FORMAT(1H ,23HTEMPERATURE PROFILE AT ,I1,I1,I1,I1,5HHOURS)
    GO TO 59
 57 WRITE(12,105) NAC,NHR,NMIN
105 FORMAT(1H ,23HTEMPERATURE PROFILE AT ,I1,I1,I2,5HHOURS)
    GO TO 59
 51 IF(NMIN.GE.9) GO TO 50
    WRITE(12,106) NHR,NAC,NMIN
106 FORMAT(1H ,23HTEMPERATURE PROFILE AT ,I2,I1,I1,5HHOURS)
    GO TO 59
 50 WRITE(12,201) NHR,NMIN
201 FORMAT(1H ,23HTEMPERATURE PROFILE AT ,2(I2),5HHOURS )
 59 WRITE(12,213) DT
213 FORMAT(1HO,21HITERATION INTERVAL IS ,F4.0,7HSECONDS)
    WRITE(12,202) TA(1),QC
202 FORMAT(1HO,25HSURFACE TEMPERATURE TA = ,F6.3,10X,
   433HSURFACE HEAT FLOW IN PROFILE A IS ,F15.10  )
    WRITE(12,203) TB(1),QD
203 FORMAT(1H ,20X,5HTB = ,F6.3,10X,
   533HSURFACE HEAT FLOW IN PROFILE B IS ,F15.10  )
    WRITE(12,204) ST
204 FORMAT(1HO,33HSURFACE TEMPERATURE DIFFERENCE = ,F6.3 )
    WRITE(12,205)
205 FORMAT(1HO)
    WRITE(12,206)
206 FORMAT(1HO,4(4X,5HDEPTH,4X,6HTEMP A,5X,6HTEMP B ))
    WRITE(12,207)
207 FORMAT(1H )
    MAN=M/4
    MAB=MAN*4
    KA=M-MAB
    DO 52 NIN=1,MAN
    MDA=NIN
    MMA=MDA
    IF(KA.GE.1) MMA=MMA&1
    MDB=MMA&MAN
    MMB=MDB
    IF(KA.GE.2) MMB=MMB&1
    MDC=MMB&MAN
    MMC=MDC
    IF(KA.GE.3) MMC=MMC&1
    MDD=MMC&MAN
```

```
   52 WRITE(12,208) MDA,TA(MDA),TB(MDA),MDB,TA(MDB),TB(MDB),
     9MDC,TA(MDC),TB(MDC),MDD,TA(MDD),TB(MDD)
  208 FORMAT(1H ,4(5X,I3,5X,F6.3,5X,F6.3))
      WRITE(12,207)
      MDA=MDA&1
      MDB=MDB&1
      MDC=MDC&1
      IF(KA.GE.3) GO TO 55
      IF(KA.GE.2) GO TO 54
      IF(KA.GE.1) GO TO 53
      GO TO 61
   55 WRITE(12,211) MDC,TA(MDC),TB(MDC)
  211 FORMAT(1H+,65X,I3,5X,F6.3,5X,F6.3)
   54 WRITE(12,210) MDB,TA(MDB),TB(MDB)
  210 FORMAT(1H+,35X,I3,5X,F6.3,5X,F6.3)
   53 WRITE(12,209) MDA,TA(MDA),TB(MDA)
  209 FORMAT(1H+,5X,I3,5X,F6.3,5X,F6.3)
      WRITE(12,205)
      WRITE(12,205)
C     END OF PRINTOUT ROUTINE
   61 CONTINUE
      IF(CMIN.LT.EMIN) GO TO 63
      IF(CHR.LT.EHR) GO TO 63
      IF(DAY.LT.EDAY) GO TO 63
      GO TO 62
   63 CONTINUE
      TIME=0.0
   40 CONTINUE
C     CALCULATION OF NEW TIME
      TIME=TIME&60.0
      CMIN=CMIN&DT/60
      IF(CMIN.LT.60.) GO TO 35
      CMIN=CMIN-60.0
      CHR=CHR&1.0
      IF(CHR.LT.24) GO TO 35
      CHR=CHR-24
      DAY=DAY&1
   35 CONTINUE
      GO TO 30
   62 CONTINUE
      KKK=KKK&1
      IF(KKK.LE.IJ) GO TO 60
      END
```

```
      SUBROUTINE QHEAT (QA,QB,QC,QD,DT,DX,TA,TB,J,K,M,CHR,CMIN,TAI)
      DIMENSION TA(120),TB(120),K(120)
      SIG=0.000136
      AMIN=CMIN/60.
      AHR=CHR&AMIN
      TAU=AHR-6.00
C     CONVERSION OF TEMPERATURES IN DEGREES CENTIGRADE TO
C     DEGREES KELVIN
      TTE=(TAI&273.16)/100
      TTR=SIG*TTE**4
      TTC=(TA(1)&273.16)/100.
      TTD=(TB(1)&273.16)/100.
C     CALCULATION OF SURFACE HEAT LOSS TERM
      QC=-(SIG*TTC**4-TTR)
      QD=-(SIG*TTD**4-TTR)
C     CALCULATION OF SURFACE HEAT FLUX
      IF(TAU.LE.0.0) GO TO 72
      IF(TAU.GE.12.0) GO TO 72
      QC=0.0055*SIN(TAU*3.14159/12)&QC
      QD=0.0055*SIN(TAU*3.14159/12)&QD
   72 CONTINUE
      RETURN
      END
```

LITERATURE CITED

1. Carslaw, H. S., and Jaeger, J. C., Conduction of Heat in Solids, 2nd ed., Clarendon Press, Oxford, 1959.

2. Carson, J. E., Technical Report ANL-6470, Argonne, Ill., Nov. 1961.

3. Cartwright, K., Illinois State Geological Survey Circular 433, Urbana, Ill., 1968.

4. Dusinberre, G. M., Heat-Transfer Calculations by Finite Differences, International Textbook Co., Scranton, 1961.

5. Fleagle, R. G., J. Meteorol., 7, 144 (1950).

6. Geiger, R., The Climate Near the Ground, Harvard University Press, Cambridge, 1965.

7. Kirkham, D., and Powers, W. L., Advanced Soil Physics, John Wiley and Sons, Inc., New York, 1972.

8. Koshlyakov, N. S., Smirnov, M. M., and Gliner, E. B., Differential Equations of Mathematical Physics, North-Holland Publishing Co., Amsterdam, 1964.

9. Lettau, H. H., and Davidson, B., Ed., Exploring the Atmosphere's First Mile, Vol. 2, Pergamon Press, London, 1957.

10. Lumsdaine, E., Engr. Exp. Sta. Bull. 17, Brookings, So. Dak., Nov. 1970.

11. Meinzer, O. E., in Ground Water and Wells, Briggs, G. F., and Fiedler, A. F., Ed., E. E. Johnson Inc., St. Paul, Minn., 1966, Chapter 1.

12. Moore, D. G., and Myers, V. I., Technical Report RSI 72-06, Brookings, So. Dak., Feb. 1972.

13. Myers, G. E., Analytical Methods in Conduction Heat Transfer, McGraw-Hill Book Co., New York, 1971.

14. Myers, V. I., NASA Report MSC-03742, Houston, Texas, Dec. 1970, Section 48.

15. Özisik, M. N., Boundary Value Problems of Heat Conduction, International Textbook Co., Scranton, 1968.

16. Smith, R. W. Jr., Technical Report RSL 69-4, Stanford, Calif., July 1969.

17. Sutton, O. G., Micrometeorology, McGraw-Hill Book Co., New York, 1953.

18. Vries, D. A. de, in Physics of Plant Environment, Wijk, W. R. van, Ed., North-Holland Publishing Co., Amsterdam, 1963.

19. Wexler, H., Mon. Wea. Rev., 64, 122 (1936).

20. Wijk, W. R. van, and Derksen, W. J., in Physics of Plant Environment, Wijk, W. R. van, Ed., North-Holland Publishing Co., Amsterdam, 1963.